J. Nannoplankton Res., **42**(1), 2024, pp. 13–35 https://doi.org/10.58998/jnr30649
 ISSN 1210-8049 Printed by The Sheridan Press, USA

Nannoconus fragilis and *Nannoconus quadriangulus*: Taxonomic and biostratigraphic revision from Aptian–Albian sections in Brazil

Cleber Fernandes Alves*
Laboratório de Palinofácies e Fácies Orgânica (LAFO-UFRJ). Av. Athos da Silveira Ramos, 274. Bloco J, sala J1 -014
Departamento de Geologia. Instituto de Geociências. CCMN. Universidade Federal do Rio de Janeiro. Cidade Universitária, Ilha do Fundão. Rio de Janeiro, RJ. Brazil. 21941-916; alvescf@gmail.com

Francisco Henrique de Oliveira Lima
PETROBRAS/CENPES, Av. Horácio Macedo, 950, Q7, Escritório 7. Cidade Universitária, Ilha do Fundão, Rio de Janeiro, RJ, Brazil. 21941-915

João Graciano Mendonça Filho
Laboratório de Palinofácies e Fácies Orgânica (LAFO-UFRJ). Av. Athos da Silveira Ramos, 274. Bloco J, sala J1 -014
Departamento de Geologia. Instituto de Geociências. CCMN. Universidade Federal do Rio de Janeiro. Cidade Universitária, Ilha do Fundão. Rio de Janeiro, RJ. Brazil. 21941-916

*Corresponding author

Manuscript received 03 June 2023; revised manuscript accepted 24 August 2023
Available online 24 April 2024
DOI: 10.58998/jnr3064

Abstract We present a comprehensive morphometric and biostratigraphic analysis of *Nannoconus* specimens obtained from 38 wells drilled by PETROBRAS along the Brazilian continental margin. The morphometric analysis of 107 specimens of *Nannoconus fragilis*, *N. quadriangulus quadriangulus*, and *N. quadriangulus apertus* resulted in the identification of parameters allowing better separation of the taxa based on their original definitions and later emendations. This study suggests that *N. quadriangulus quadriangulu*s and *N. quadriangulus* apertus are restricted to the Aptian, as their geological range is directly correlated with the interval encompassed by the *Globigerinelloides ferreolensis* and *Paraticinella rorhi* foraminifera biozones. *Nannoconus fragilis* appears to be limited to the Albian as it consistently occurs within the *Microhedbergella renilevis* through *Ticinella primula* foraminifera biozones. The biochronostratigraphic distribution of these taxa along the Brazilian margin is consistent with previous studies from other regions.

Keywords Calcareous nannofossils, nannoconids, morphometric analysis, Early Cretaceous, South Atlantic Ocean

1. Introduction

Recent studies of several Cretaceous sections from the Brazilian continental margin (Alves et al., 2017; Lima et al., 2018, 2019; Viviers et al., 2018; Sanjinés et al., 2019, 2022) have shown the importance of a more detailed study of some *Nannoconus* species that are significant biostratigraphic markers and paleoecological indicators for the Early Cretaceous. This is particularly true for Brazilian sedimentary basins where those nannofossils are used to provide a regional biostratigraphic framework and paleoecological reconstructions across the Aptian and Albian intervals (Troelsen & Quadros, 1971; Cunha, 1990a,b; Antunes, 1996; Cunha & Shimabukuro, 1997; Cunha & Koutsoukos, 1998; Alves et al., 2017).

In this investigation, the species *Nannoconus fragilis*, *N. quadriangulus quadriangulus*, and *N. quadriangulus apertus* were re-evaluated from a morphometric point of view. The analyzed material comes from the Aptian and Albian carbonate to mixed post-salt section in 38 wells drilled by PETROBRAS along the Brazilian continental margin. These nannofossils were selected due to the need to better understand their taxonomy, chronostratigraphic distribution, and potential biostratigraphic value in the Aptian–Albian interval. Using previous studies, morphometric analyses, and new taxonomic criteria, this study contributes to the development and improvement of a biostratigraphic framework for the Aptian–Albian of the Brazilian continental margin.

2. Historical studies of *Nannoconus*

2.1. Morphometric studies

Brönnimann (1955) built on the first studies of *Nannoconus* (de Lapparent, 1925; Kamptner, 1931, 1938; Colom, 1945) to establish a classification based on their morphological attributes. The diagnostic characteristics of the group observed in longitudinal sections of the specimens included the outline and dimensions of the test, central opening and presence of a canal (<1 μm aperture) or cavity (>1 μm), thickness and composition of the walls, and position and diameter of the apertures (apical and basal). Brönnimann (1955) also considered the cross sections (plan view) of the nannoconids to better characterize the central canal (<1 μm) or cavity (>1 μm) and wall thickness and structure.

Trejo (1960) confirmed the revision of Brönnimann (1955), particularly the characteristics of the thickness and structure of walls. The author also highlighted the use of cross-polarized light under the optical microscope for better resolution of specific structures, such as the spiral lines of the walls in longitudinal view. In the same work, Trejo (1960) established a classification key for some nannoconid species (*N. steinmannii, N. bermudezi*, *N. elongatus*, *N. bronnimannii*, *N. minutus*, *N. truittii*, *N. globulus*, *N. bucheri*, *N. kamptneri*, *N. colomii*, *N. wassallii*, and *N. bonetii*) based on multiple combinations of the morphology of the central opening (spherical, suboval, subcone, piriform, globular, or cylindrical), morphology of the outline of the nanoconnid (conical, circular, suboval, piriform, subrectangular, or rectangular), proportion of the diameter of the central opening to the wall thickness, and proportion of the length to the maximum width of the test.

Báldi-Beke (1962) considered the outline of the test and the central opening as the most important criteria for the taxonomic determination of nannoconids. The works of Noël (1959, 1965) proposed as a biometric parameter the ratio between the maximum and the minimum diameter of some nannoconids (*N. steinmanni*, *N. colomi*, *N. kamptneri*, *N. bermudezi*, *N.* cf. *N. globulus*, *N. elongatus*, *N. truittii*, *N. wassalli*, and *N. bucheri*). Deflandre & Deflandre-Rigaud (1962, 1967) studied some Aptian nannoconids (*N. carniolensis*, *N. calpidomorphus*, *N. boletus boletus*, *N. boletus curtus*, *N. inconspicuus*, *N. quadriangulus*, and *N. quadriangulus apertus*). The authors applied the diagnostic features proposed by Brönnimann (1955) and Trejo (1960), together with the width and the type of aperture at the poles. These characteristics were also later used by Barrier (1977).

Bouché (1965) used only four of the morphological attributes used previously by Trejo (1960) and Deflandre & Deflandre-Regaud (1962) to discriminate various species of *Nannoconus*: outline of the test, wall thickness, morphology of the poles, and development of the central opening. Moshkovitz (1972) used these four attributes, in addition to the following parameters for biometric studies: diameter of the central opening, length of the test, maximum and minimum diameter of the test, and proportion of the diameter of the central opening to the maximum diameter of the test. Deres & Achéritéguy (1972, 1980) used some of the same morphological criteria for determination of morphogroups, including morphology of the outline of the nannoconids (piriform, conical, square, subspherical, or rectangular), proportion of the wall thickness to the width of the central opening (≤1 or >1), and proportion of the length to the maximum diameter (≥1 or <1) of the test. However, they also used the presence of a flange and, consequently, thickening or enlargement of one or both poles of the nannoconid as a key criterion.

Aubry (1974) conducted a morphometric study of several species of *Nannoconus* (*N. elongatus*, *N. minutus*, *N. multicadus*, *N. truittii truittii*, *N. dauvillieri*, and *N. farinacciae*). She used the following characteristics to discriminate different species: outline and dimensions of the test, diameter and morphology of the central opening, morphology of the poles, maximum and minimum diameter of the test, and architecture of the wall. According to van Niel (1992), the crystallography of the walls plays a fundamental role in the morphology of nannoconids. The author systematically studied characteristics of the crystals of the nannoconids, including the dimensions of the crystals, the inclination of the crystals (angles α and β), and width of the crystallographic cycles (cycles A and B) to distinguish five morphogroups.

Özkan-Altiner (1999) incorporated some characteristics of nannoconid crystallography in the revision of many *Nannoconus* species (*N. bermudezii*, *N. bonetii*, *N. bucheri*, *N. carniolensis*, *N. cornuta*, *N. elongatus*, *N. globulus globulus*, *N. grandis*, *N. inconspicuus*, *N. kamptneri kamptneri*, *N. kamptneri minor*, *N. minutus*, *N. multicadus*, *N. quadriangulus quadriangulus*, *N. quadriangulus apertus*, *N. steinmannii minor*, *N. truittii truittii*, *N. truittii frequens*, *N. vocontiensis*, and *N. wassallii*). The parameters used for species classification included external morphol-

ogy of the test, diameter of the central opening (presence of cavity or canal), morphology of the poles, proportion of the diameter of the central opening to the wall thickness of the test, proportion of the diameter of the length to the width of the test, and crystallography of the walls.

Bralower et al. (1989) and later Casellato (2010) investigated the evolution of nannoconids in the late Tithonian–earliest Berriasian based on morphological parameters such as external shape (spherical, subspherical, conical, or subconical), length, maximum width, diameter of the central opening, and size variation within individual species. Tremolada & Young (2002) and Bornemann et al. (2003) conducted studies where they estimated the volume of various calcareous nannofossils, including some *Nannoconus* species. These estimates were obtained based on calculations of the maximum and minimum diameter, diameter of the central opening, wall thickness, length, and external shape of the specimen. Most recently, Barbarin et al. (2012) used the length, width, minimum and maximum diameters, and central opening to distinguish some species of *Nannoconus*. The comparisons of the main morphometric parameters used for study of nannoconids as reported in the literature are summarized in Table 1.

Table 1: Comparison of the main morphological characteristics of nannoconids used for differentiation by various authors.

	MORPHOMETRIC ATTRIBUTES										
REFERENCES	External morphology (outline of test)	Diameter of central opening	Thickness of the wall diameter	Apertures and morphology of the poles	Morphology of central opening	Length (height)	Maximum width	Width and aperture at the poles	Maximum diameter	Minimum diameter	Crystallography of the wall
Bronnimann (1955)	•	•	•	•				•			
Trejo (1960)	•	•	•	•	•	•	•	•	•		
Baldi-Beke (1962)	•				•						
Nöel (1959, 1965)									•	•	
Deflandre & Deflandre-Rigaud (1962, 1967)	•	•	•	•	•	•	•	•			
Bouché (1965)	•		•	•	•						
Moshkovitz (1972)	•	•	•	•	•	•	•	•	•	•	
Deres & Achéritéguy (1972, 1980)	•	•	•			•	•	•	•		
Aubry (1974)	•	•		•	•	•			•	•	•
Barrier (1977)	•	•	•	•		•		•			
Bralower et al (1989)	•					•	•				
van Niel (1992)											•
Özkan-Altiner (1999)	•	•	•	•		•	•	•			•
Tremolada & Young (2002)	•	•	•			•			•	•	
Bornemann et al. (2003)	•	•	•			•			•	•	
Casellato (2010)	•					•	•				
Barbarin et al. (2012)		•				•	•		•	•	

2.2. Biostratigraphic studies

Nannoconus fragilis and the subspecies of *Nannoconus quadriangulus* have been identified in many mid-Cretaceous sections from around the world. Here we briefly summarize studies documenting these taxa, followed by a summary of studies from the Brazilian margin (Figure 1).

2.2.1 *Nannoconus fragilis*

The species *N. fragilis* was described by Deres & Achéritéguy (1980); however, it was previously illustrated by Deres & Achéritéguy (1972) as "*Nannoconus* sp. 93" and its stratigraphic distribution attributed exclusively to the Albian. Perch-Nielsen (1985) also indicated an Albian stratigraphic distribution and presented illustrations of *N. fragilis*. Lambert & Laporte-Galaa (1996) suggested two evolutionary schemes for *N. quadriangulus* and *N. fragilis*. The first hypothesized an evolutionary transition from *N. quadriangulus* to *N. fragilis* across the Aptian/Albian boundary, with possible coexistence for a short time. The second hypothesis suggested a short coexistence of these nannoconids during the earliest Albian. However, in their conclusions, Lambert & Laporte-Galaa (1996) adopted the biostratigraphic distribution of Deres & Achéritéguy (1980), with *N. quadriangulus* restricted to the Aptian and *N. fragilis* to the Albian. In the Nannotax database (Young et al., 2023), *N. fragilis* is included in the *Nannoconus circularis* group and its geological range is restricted to the Albian, following Perch-Nielsen (1985).

Kaiser-Weidich & Schairer (1990), in an integrated study including ammonites, calpionellids, and nannoconids in the Northern Alps (Switzerland), inferred an Albian age for *N. fragilis*. Kennedy et al. (2000) presented an integrated stratigraphy of the Aptian–Albian interval in sections from France with a sporadic distribution of nannoconids. They suggested that their occurrence and preservation were probably controlled by paleoenvironmental factors such as changes in temperature and/or surface water productivity. *Nannoconus fragilis* was only listed in the nannofossil distribution charts and present in a few Albian samples in that study. Jeremiah (2001) proposed a biozonation based on nannofossils from the Lower Cretaceous of the North Sea Basin. He reported sporadic occurrences of poorly preserved *N. fragilis* in a few Barremian/Aptian samples; however, he did not include any illustrations of *N. fragilis*. Herrle (2003) and Bornemann et al. (2005) identified *N. fragilis* in the lower Albian of the Vocontian Basin (France) in association with other nannoconids.

Verdenius (1993) reported the occurrence of *N.*

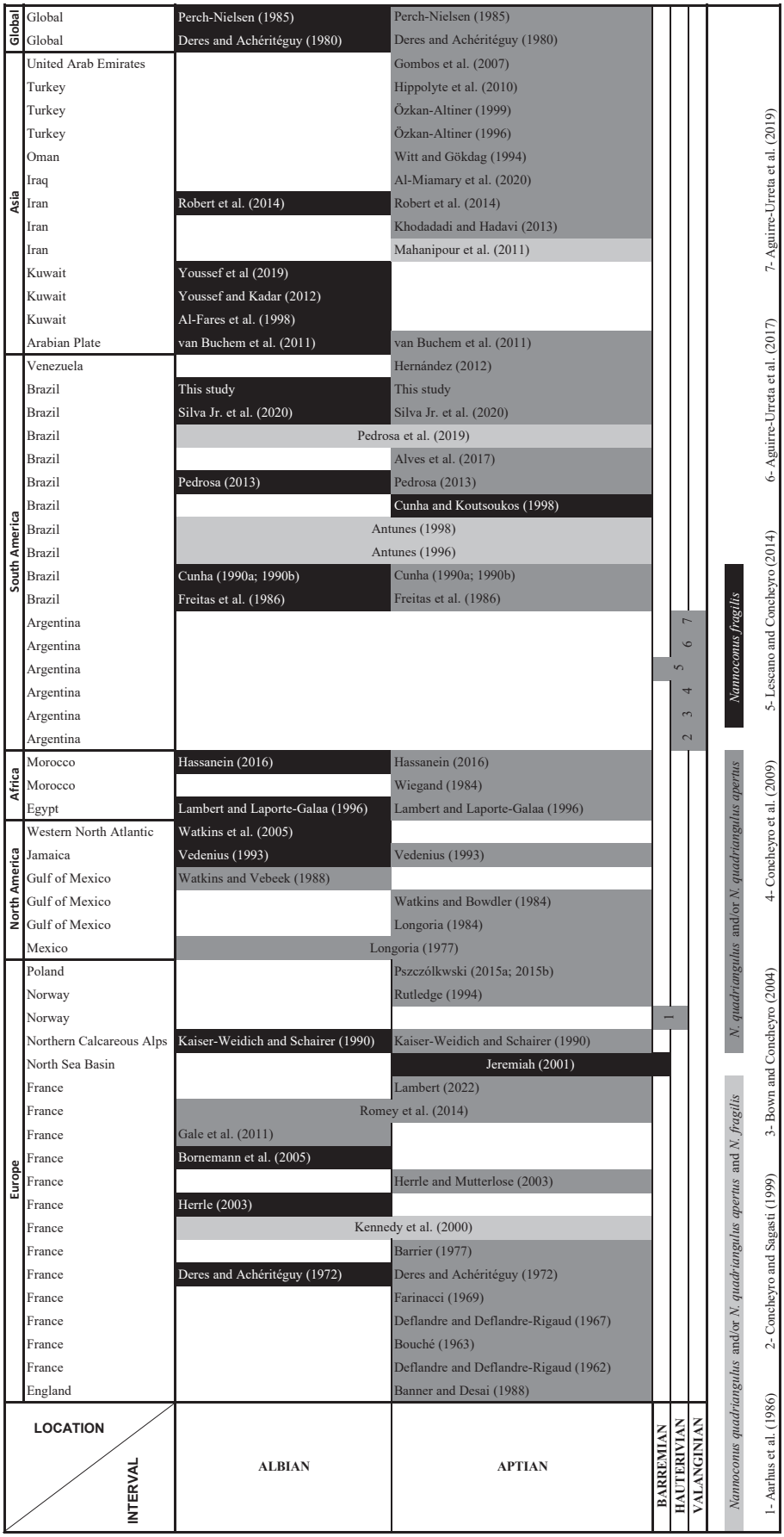

Figure 1: Summary of biostratigraphic studies of *Nannoconus fragilis* and *N. quadriangulus* by age and region (see text for details).

fragilis in sediments from the Campanian section of St. Ann's Great River (Jamaica) and considered *N. fragilis* as a reworked Albian nannofossil. Watkins et al. (2005) correlated calcareous nannofossil events with the stable isotope record in a Cretaceous section of Ocean Drilling Program (ODP) Hole 1052E (Blake Nose, western North Atlantic). In that study, they identified the last occurrence of *N. fragilis* very close to the Albian/Cenomanian boundary, as previously indicated by Perch-Nielsen (1985).

Al-Fares et al. (1998) established a regional biozonation for the coast of Kuwait that also restricted the distribution of *N. fragilis* to the Albian. Mahanipour et al. (2011) recorded *N. fragilis* in the Aptian of the Kopet Dagh Basin (Iran), although Robert et al. (2014) indicated an Albian age for the same region (NE Iran). In the Kuwait coastal area, van Buchem et al. (2011), Youssef & Kadar (2012), and Youssef et al. (2019) confirmed previous findings of Al-Fares et al. (1998) and used *N. fragilis* as an index fossil for the Albian. Hassanein (2016) recorded rare occurrences of *N. fragilis* in the Albian interval of an Aptian–Albian outcrop section in the Agadir-Essaouira Basin (Morocco).

2.2.2. *Nannoconus quadriangulus*

Nannoconus quadriangulus is represented by the subspecies *N. quadriangulus quadriangulus* and *N. quadriangulus apertus*, although some studies do not distinguish between the two subspecies.

Nannoconus quadriangulus and *N. quadriangulus apertus* were described by Deflandre & Deflandre-Rigaud (1962), where their holotypes were represented by illustrations. The diagnoses of the species were later published by Deflandre & Deflandre-Rigaud (1967). Bouché (1963) identified *N. quadriangulus* and *N. quadriangulus apertus* in his work on the nannoconids of the Early Cretaceous and Farinacci (1969) compiled the information of Deflandre & Deflandre-Rigaud (1962, 1967). Deres & Achéritéguy (1972) summarized the chronostratigraphic distribution of many species of *Nannoconus* and indicated a late Aptian age for *N. quadriangulus quadriangulus* and *N. quadriangulus apertus*. Barrier (1977) confirmed the descriptions of Deflandre & Deflandre-Rigaud (1967) for *N. quadriangulus* and recorded the two subspecies in the upper Aptian in southeast France. Longoria (1977) proposed a biostratigraphic framework for the Early Cretaceous of the Nuevo León region (Mexico) in which *N. quadriangulus* is present from the lower Aptian to the upper Albian. Deres & Achéritéguy (1980) presented a global stratigraphic scheme based on nannoconids and reaffirmed the morphological classification and biostratigraphy proposed in Deres & Achéritéguy (1972). Perch-Nielsen (1985) followed the scheme of Deres & Achéritéguy (1980) for her illustrations, terminology, and stratigraphic distribution of *N. quadriangulus quadriangulus* and *N. quadriangulus apertus*, indicating a distribution restricted to the Aptian. According to the Nannotax database (Young et al., 2023), *N. quadriangulus quadriangulus* and *N. quadriangulus apertus* are included in the *Nannoconus truittii* group and their geological range is restricted to the Aptian, following Perch-Nielsen (1985).

Since the original descriptions of *N. quadriangulus* and *N. quadriangulus apertus* were published and initial work conducted to delineate their stratigraphic occurrence, there have been many studies that identify these taxa in outcrops and marine sediments from around the world. Watkins and Bowdler (1984) reported the occurrence of *N. quadriangulus* in the Gulf of Mexico (Deep Sea Drilling Project [DSDP] Site 535) in the upper Aptian. Longoria (1984) established a Cretaceous biochronology for the Gulf of Mexico based on planktonic microfossils and indicated the occurrence of *N. quadriangulus* as exclusively Aptian in that region. Wiegand (1984) studied the calcareous nannofossils of DSDP Site 545 (eastern Atlantic Ocean off the coast of Morocco). He indicated that *N. quadriangulus* and *N. quadriangulus apertus* are present in the lower part of the *Rhagodiscus angustus* Zone of Manivit (1971) modified by Thierstein (1973) and probably late Aptian in age. Watkins and Verbeek (1988) reported *N. quadriangulus* in the Albian interval from the Northeast Providence Channel (ODP Hole 635B, Bahamas), although this species was listed only in the distribution table. Verdenius (1993) reported *N. quadriangulus* in material from the Campanian section of St. Ann's Great River (Jamaica) and considered this occurrence as reworked from the Aptian.

Rutledge (1994) cited the occurrence of *N. quadriangulus* in an assemblage with other Aptian nannofossils including *Micrantholithus* spp. and *Farhania varolii* in the Norwegian Barents Sea. Aarhus et al. (1986) reported a single occurrence of *N. quadriangulus* in a Hauterivian–Barremian section in Norway. In a study of planktonic

foraminifera from Speeton (England), Banner & Desai (1988) reported the occurrence of *N. quadriangulus apertus* in the same section in which foraminifera indicated a late Aptian age. In an integrated study including ammonites, calpionellids, and nannoconids from the Northern Alps (Switzerland), Kaiser-Weidich & Schairer (1990) inferred an Aptian age for *N. quadriangulus quadriangulus* and *N. quadriangulus apertus*. Kennedy et al. (2000) recorded specimens of *N. quadriangulus quadriangulus* and *N. quadriangulus apertus* in a few samples from the Col du Pré-Guittard, Arnayon (Drôme) and Tartonne (Alpes-de-Haute-Provence), France. Herrle & Mutterlose (2003) reported *N. quadriangulus* in the Aptian of the Vocontian Basin (France) without distinguishing the two subspecies. On the other hand, Gale et al. (2011) identified rare specimens of *Nannoconus quadriangulus quadriangulus* and *N. quadriangulus apertus* in Albian assemblages of the Voncotian Basin. Romey et al. (2014) also found *N. quadriangulus quadriangulus* in Aptian–Albian assemblages in the Cassis region, Vocontian Basin. Pszczółkowski (2015a,b) highlighted the occurrence of *N. quadriangulus apertus* in Aptian sediments from Poland. One of the most recent publications discussing *N. quadriangulus* from European sections is from Lambert (2022), who defined biozones based on nannoconid associations from Aptian sections of the Vaucluse region in southeastern France.

Witt & Gökdag (1994) found *N. quadriangulus* in the upper Aptian Shuaiba Formation (Oman). Lambert and Laporte-Galaa (1996) adopted the biostratigraphic distribution of Deres & Achéritéguy (1980), suggesting an Aptian distribution for *N. quadriangulus* in the offshore of North Sinai, Egypt. Özkan-Altiner (1996, 1999) reported *N. quadriangulus quadriangulus* and *N. quadriangulus apertus* in Aptian deposits of northwest Anatolia, Turkey. Gombos et al. (2007) found *Nannoconus quadriangulus* in upper Aptian sections of the Shuaiba Formation (Abu Dhabi, United Arab Emirates). Hippolyte et al. (2010) recorded *N. quadriangulus quadriangulus* and *N. quadriangulus apertus* in association with *Nannoconus bucheri* and *N. circulari* in upper Aptian sediments in the Black Sea Basin (Turkey). Mahanipour et al. (2011) recorded *N. quadriangulus* in an Aptian outcrop of the Kopet Dagh Basin (Iran). Its presence in that region was later confirmed by Khodadadi & Hadavi (2013) and Robert et al. (2014). In the Bab Basin (Arabian Plate), van Buchem et al. (2011) used *N. quadriangulus* as an index fossil for the late Aptian(?), in agreement with the Witt & Gökdag (1994) record from the Shuaiba Formation (Oman). Hassanein (2016) recorded rare occurrences of *N. quadriangulus* in the Aptian of an Aptian–Albian outcrop section of the Agadir-Essaouira Basin (Morocco). Al-Miamary et al. (2020) carried out a study involving calcareous nannofossils and chemostratigraphy of the Balambo Formation (northern Iraq), where the authors observed the occurrence of *N. quadriangulus* in the lower Aptian.

Concheyro & Sagasti (1999) identified *N. quadriangulus quadriangulus* from the Valanginian to Hauterivian interval of the Neuquén Basin, Argentina. Similarly, Bown & Concheyro (2004) reported the occurrence of *N. quadriangulus quadriangulus* and *N. quadriangulus apertus* from the Valanginian to Hauterivian of the Neuquén Basin. Lescano & Concheyro (2014) and Aguirre-Urreta et al. (2017, 2019) suggested that *N. quadriangulus apertus* evolved in the Valanginian due to its presence in the Vaca Muerta and Agrio Formations (Neuquén Basin, Argentina), which were dated as Valanginian–Barremian (Lescano and Concheyro, 2014) and later updated to Valanginian–Hauterivian (Aguirre-Urreta et al., 2017, 2019). Hernández (2012) studied the "Río Frío - Cerro las Minas" area in Venezuela. He found *N. quadriangulus apertus*, *N. boletus*, *N. wassallii*, and *N.* cf. *vocontiensis* in the Apón Formation and interpreted an Aptian age for this section based on these species and other fossils (palynomorphs, planktonic foraminifera, and bivalves).

2.2.3. *Nannoconus fragilis* and *Nannoconus quadriangulus* in Brazil

Freitas et al. (1986) noted the difficulty in identifying and separating *N. quadriangulus* and *N. fragilis* in Brazilian continental margin sediments. The authors published a short review regarding specimens of *N. quadriangulus apertus* and *N. fragilis* of the Sergipe-Alagoas Basin, dated as Aptian–Albian. Cunha (1990a) followed Deres & Achériteguy (1980) in separating *N. fragilis* and *N. quadriangulus apertus* in the Ceará Basin, Brazil. In this work and Cunha (1990b), the author proposed the *Nannoconus fragilis* Zone of Aptian–Albian age, with the top of the zone defined by the last occurrence of the nominative species. Cunha (1990a) specified an Aptian age for the basal part of the *Nannoconus fragilis* Zone based on the presence of *N. quadriangulus apertus*. However, he did not define the base of the zone as it was the oldest unit in

the studied section, and he used interval zones formed by two successive last occurrences in his biozonation.

Cassab et al. (1994) mentioned the occurrence of *N. fragilis* and *N. quadriangulus* in the taxonomic list for the Sergipe-Alagoas Basin, without further details. Antunes (1996, 1998) proposed a biostratigraphic framework for the Brazilian continental margin in which he assigned the code "N-240" for the *Nannoconus fragilis* Zone and emended the zone to define its base by the first occurrence of *N. fragilis*. In addition, these publications reviewed the history of difficulties in taxonomic recognition and noted a lack of more in-depth knowledge of nannoconids, again highlighting the close relationship between *N. quadriangulus apertus* and *N. fragilis*.

Cunha & Koutsoukos (1998), in a study making paleoecological inferences using nannofossils and planktonic foraminifera of the Aptian of the Sergipe Basin, mentioned the species *N. fragilis* in the distribution chart. In the same basin, Pedrosa (2013) recorded the occurrence of *N. fragilis* and *N. quadriangulus* as being Aptian–Albian age. Alves et al. (2017) identified the occurrence of *N. quadriangulus quadriangulus* and *N. quadriangulus apertus* in an interval considered Aptian for some basins of the Brazilian continental margin. Pedrosa et al. (2019) associated the occurrence of *N. fragilis* and *N. quadriangulus apertus* as Albian in cuttings samples (Hole A1SE) from the Sergipe Basin (Brazil). Silva et al. (2020) observed *N. fragilis* and *N. quadriangulus* in the Albian section of a cored well from the Sergipe-Alagoas Basin (Brazil); however, the *N. quadriangulus* specimens were considered reworked.

3. Material and methods

The samples analyzed in this study come from 38 wells drilled by PETROBRAS along the Brazilian continental margin (Figure 2). More details about the Brazilian sedimentary basins can be found in Milani et al. (2007).

Calcareous nannofossil samples were prepared as smear slides following the technique described in Bown & Young (1998). Smear slides were examined using a Zeiss Axio Imager A2 polarizing light microscope at 1600× magnification. Images were taken under cross-polarized light (XPL), brightfield (BF), and with a gypsum plate (GP), and captured using AxioVision 40x64 v. 4.9 Zeiss software. Images and slides were deposited in the collection of the Biostratigraphy and Paleoecology Research and Development Centre, PETROBRAS/CENPES/PDIEP/IGEO/BPA.

We adopted the nannoconid taxonomy of Deres & Achéritéguy (1980), Perch-Nielsen (1985), van Niel (1992, 1994), and Young et al. (1997, 2023). The morphometric analysis of nannoconids was based on the morphological characteristics described by Brönnimann (1955), Trejo (1960), Deflandre & Deflandre-Rigaud (1962), Bouché (1963, 1965), Deres & Achéritéguy (1972, 1980), Moshkovitz (1972), van Niel (1992), and Özkan-Altiner (1999) (Figure 3). A total of 107 specimens were analyzed in longitudinal view and six selected morphometric characteristics were measured: maximum diameter (MD), height (H), central opening (CO), wall thickness (WT), base (B), and apex (A). Statistical parameters were calculated using PAST software (Hammer et al., 2001). For biostratigraphic interpretation, the biozonations of Sissingh (1977), Perch-Nielsen (1985), and Bown (1998) were used. Most bibliographic references can be found in Perch-Nielsen (1985), Bown (1998), and Young et al. (2023).

4. Results

Nannofossils in the studied sections are common to abundant and are well preserved. Selected specimens of each species are illustrated in Plate 1. The biochronostratigraphic calibration was based on planktonic foraminifera analyzed in the same wells investigated in this study (Lima et al., 2018, 2019; Viviers et al., 2018; Sanjinés et al., 2019, 2022). The common nannofossil assemblages observed in the Brazilian continental margin wells and their correlations with planktonic foraminiferal biozones are shown in Table 2.

4.1. Biometric analysis

As previously mentioned, several studies have recognized the difficulty in identifying and separating *Nannoconus quadriangulus* and *N. fragilis*. To solve this problem, we carried out morphometric analyses of longitudinal sections using the main characteristics illustrated in Figure 4. The morphological parameters and the ratio between them were selected according to previous studies (holotypes and subsequent papers), as described above in Section 2.1 (Morphometric studies) and Table 1.

The morphology of a total of 107 individual nannoconids (identified according to the literature as *Nannoconus fragilis*, *N. quadriangulus quadriangulus*, and *N. quadri-*

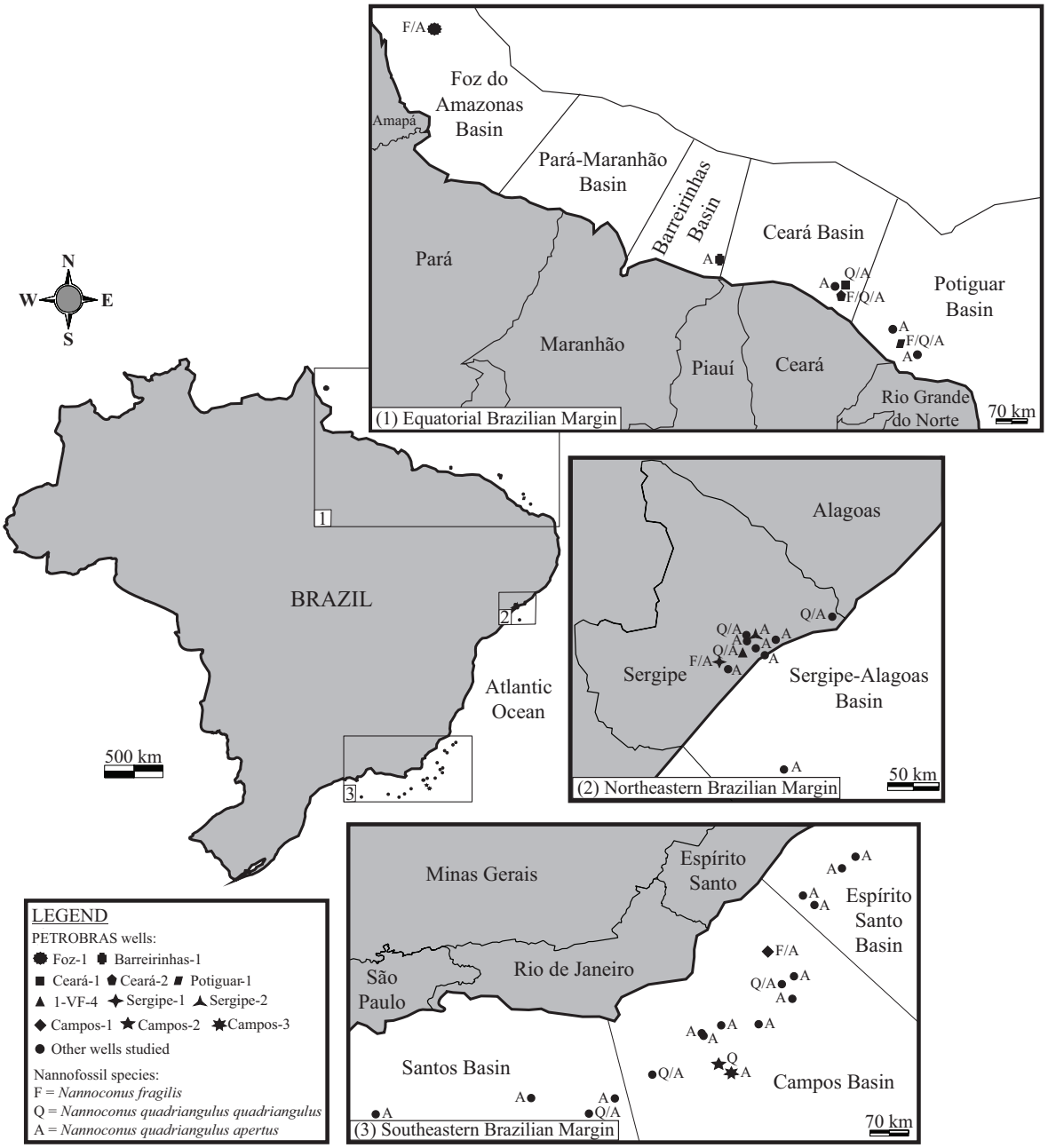

Figure 2: Location map showing the distribution of the 38 studied wells in the Brazilian sedimentary basins and presence of *Nannoconus fragilis*, *N. quadriangulus quadriangulus*, and *N. quadriangulus apertus*. Exact locations of wells are proprietary.

angulus apertus) was analyzed by measuring the maximum diameter, height, central opening, wall thickness, base, and apex (Figure 4; Table 3; Appendix 1). We used frequency histograms and gaussian Kernel density plots, as well as box plots, to analyze all measured parameters for each studied species (Figures 5 and 6).

4.1.1. Maximum diameter and height

Nannoconus quadriangulus apertus shows a smaller size (mean MD = 5.99 µm; mean H = 4.05 µm) compared to *N. fragilis* (mean MD = 6.69 µm; mean H = 4.74 µm) and *N. quadriangulus quadriangulus* (mean MD = 6.98 µm; mean H = 5.47 µm) (Table 3; Figures 5A, 5B, and 6A). When analyzing the ratio between the maximum diameter and the height of these nannoconids, it is possible to identify two patterns: *N. fragilis* and *N. quadriangulus apertus* show very similar values (mean MD/H of 1.41 µm and 1.47 µm, respectively) and *N. quadriangulus quadriangulus* has a lower average ratio (mean MD/H = 1.27 µm).

4.1.2. Central opening and wall thickness

The size variations of the central opening and wall thick-

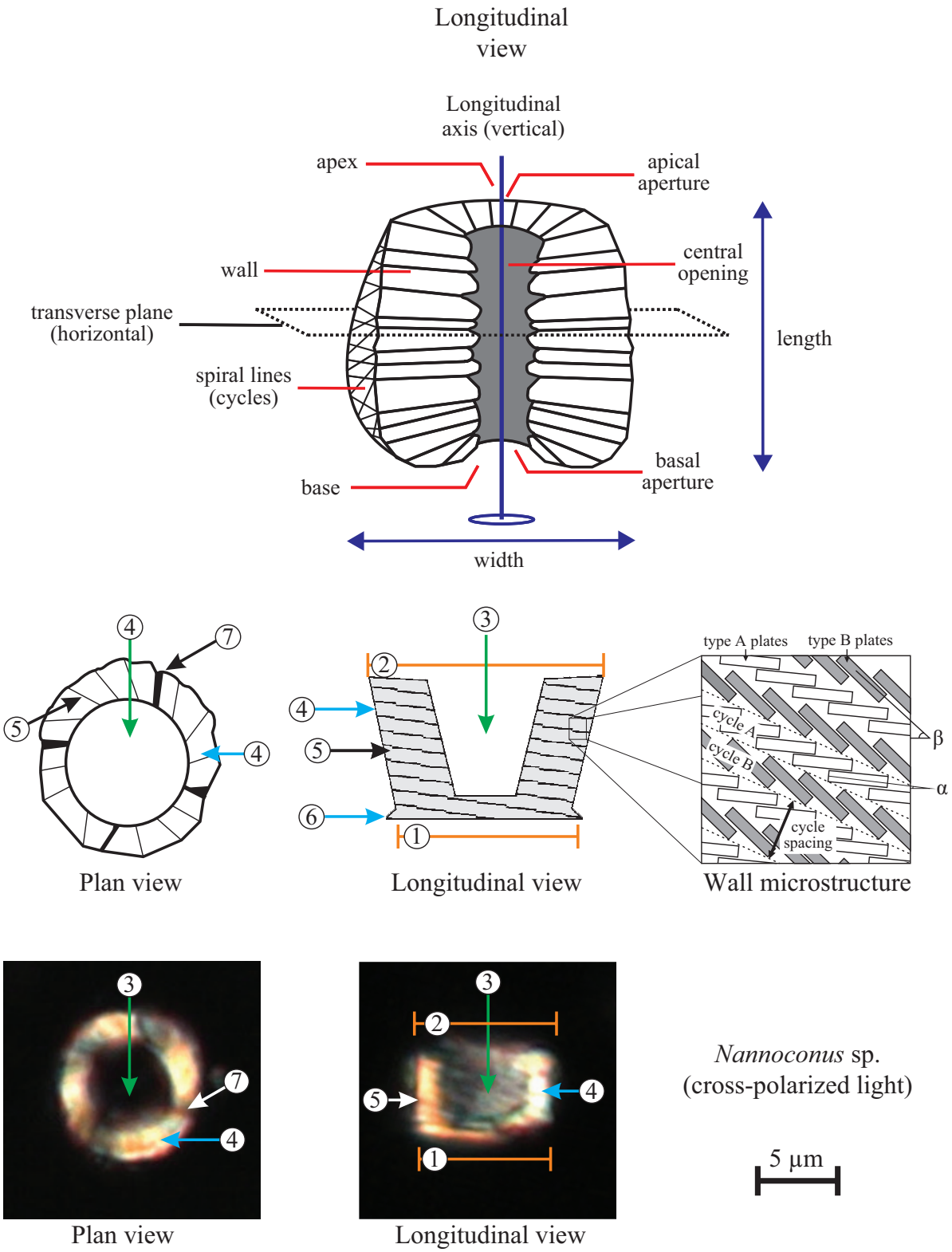

Figure 3: Schematic drawings and photomicrographs of *Nannoconus* showing the general structure of the studied species and terminology used (modified from Brönnimann, 1955; van Niel 1992, 1994; Young et al., 1997; Özkan-Altiner, 1999).

Table 2: Nannofossil assemblages and their correlations with foraminiferal biozones from the studied wells on the Brazilian continental margin.

Studied nannoconids	Specific co-occurrences	Common taxa identified	Planktonic foraminifera biozones
Nannoconus fragilis	*Axopodorhabdus albianus* *Prediscosphaera columnata* *Prediscosphaera cretacea*	*Biscutum constans, Braarudosphaera africana, Braarudosphaera regularis, Chiastozygus litterarius, Eprolithus floralis, Flabelites oblongus, Hayesites irregularis, Helenea chiastia, Lithraphidites carniolensis, Manivitella pemmatoidea, Microrhabdulus primitivus, Nannoconus elongatus, Nannoconus truittii, Radiolithus planus, Retecapsa crenulata, Rhagodiscus achlyostaurion, Rhagodiscus angustus, Rhagodiscus asper, Rucinolithus terebrodentarius youngii, Tetrapodorhabdus decorus, Tranolithus gabalus, Watznaueria barnesiae, Watznaueria britannica, Watznaueria supracretacea, Zeugrhabdotus diplogrammus, Zeugrhabdotus embergeri, Zeugrhabdotus erectus, Zeugrhabdotus noeliae, Zeugrhabdotus xenotus*	*Microhedbergella renilevis – Ticinella primula*
Nannoconus quadriangulus quadriangulus **and/or** ***Nannoconus quadriangulus apertus***	*Braarudosphaera batilliformis* *Braarudosphaera pseudobatilliformis* *Micrantholithus hoschulzii* *Nannoconus bucheri* *Nannoconus circularis* *Nannoconus globulus* *Nannoconus troelsenii* *Rucinolithus infracretacea larsonnii*		*Globigerinelloides ferreolensis – Paraticinella rorhi*

ness are notable in *N. quadriangulus quadriangulus*. The specimens of this subspecies show the lowest mean central opening size (3.27 µm) and the highest mean wall thickness (2.14 µm) among the species studied (*N. quadriangulus apertus*: mean CO = 3.63 µm; mean WT = 1.26 µm; *N. fragilis*: mean CO = 4.00 µm; mean WT = 1.37 µm) (Table 3; Figures 5E, 5D, and 6B). The ratio between the central opening and wall thickness is very similar for *N. fragilis* and *N. quadriangulus apertus* (mean CO/WT of 2.92 µm and 2.88 µm, respectively), whereas the ratio for *N. quadriangulus quadriangulus* is consistently less than 2 µm (mean CO/WT of 1.53 µm). Therefore, the ratio of the central opening to the wall thickness can be used to differentiate the species as follows: CO/WT ≥ 2 µm for *N. fragilis* and *N. quadriangulus apertus* and CO/WT < 2 µm for *N. quadriangulus quadriangulus*.

4.1.3. Base and apex width

The histograms of the base and apex sizes (Figures 5E and 5F) do not show significant differences among the analyzed taxa. However, by following previous studies and comparing the values obtained in our morphometric investigation, the base-apex relationship displays small differences that can be useful (*N. fragilis*: mean B = 6.67 µm, A = 5.98 µm; *N. quadriangulus quadriangulus*: mean B = 6.90 µm, A = 6.95 µm; *N. quadriangulus apertus*: mean B = 5.31 µm, A = 5.99 µm), as illustrated in Table 3 and Figures 6C and 7. The morphometric analysis of the base width/apex width allows us to separate the specimens into the three taxa, where *N. fragilis* is characterized by a base wider than the apex (mean B/A = 1.11 µm), *N. quadriangulus quadriangulus* has a base approximately equal to the apex (mean B/A = 0.99 µm), and *N. quadriangulus apertus* shows a base narrower than the apex (mean B/A = 0.89 µm) (Figures 6C and 7).

4.2. Statistical treatment

We used a simple linear regression (Figure 8) and principal component analysis (PCA) (Table 4) to validate the relationships among the selected morphometric parameters. The scatter plot between the base and apex widths shows extremely good correlation (r = 0.944) (Figure 8A) and good correlation also exists between the maximum diameter and height (r = 0.906) (Figure 8B). The correlation between wall thickness and central opening instead shows a low correlation coefficient (r = 0.510) (Figure 8C). According to Nöel (1965), Moshkovitz (1972), and Casellato (2010), diagenetic alteration of nannoconids can interfere

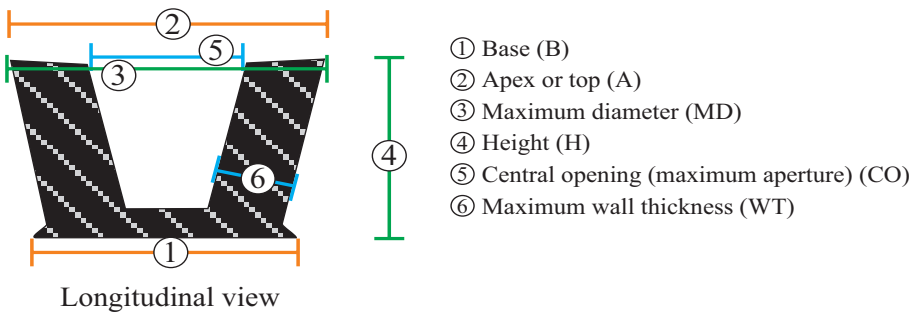

Figure 4: Morphological characteristics measured in this study (in longitudinal view) shown on a schematic drawing of *Nannoconus*.

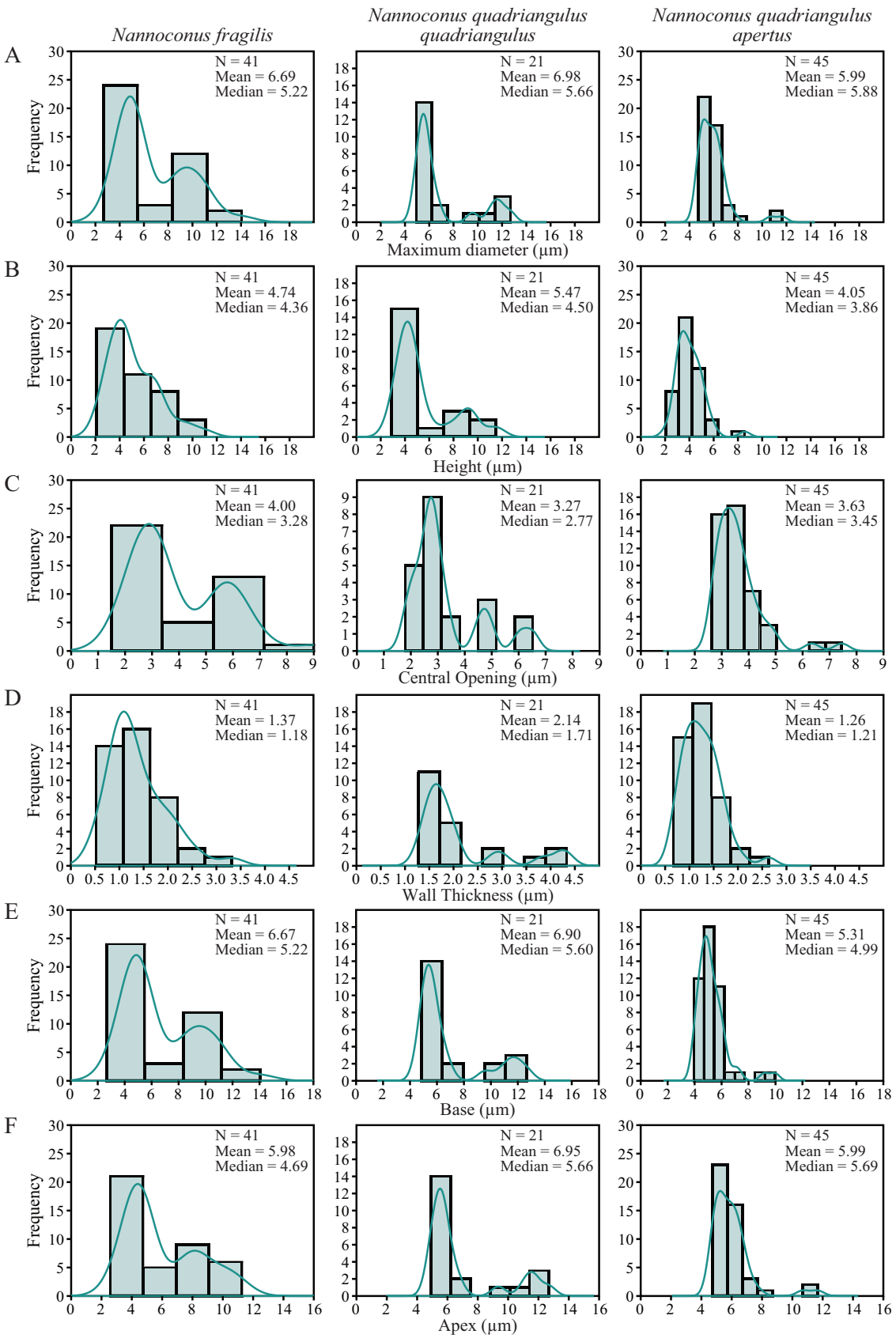

Figure 5: Frequency histograms and gaussian Kernel density plots applied to all measured parameters. Total number of specimens examined, as well as the mean and median value for each measurement are shown in the upper righthand corner of each plot. Frequency distribution of (A) maximum diameter, (B) height, (C) central opening, (D) wall thickness, (E) base, and (F) apex for *Nannoconus fragilis* (left column), *N. quadriangulus quadriangulus* (middle column), and *N. quadriangulus apertus* (right column).

Table 3: Biometrics parameter statistics for all *Nannoconus* specimens studied. MD = maximum diameter, H = height, CO = central opening, WT = wall thickness, B = base, A = apex.

		MD	H	CO	WT	B	A
ALL SPECIMENS	Number of specimens (N)	107	107	107	107	107	107
	Minimum (µm)	2.66	2.04	1.5	0.52	2.66	2.58
	Maximum (µm)	14.05	11.49	9.05	4.33	14.05	12.7
	Mean (µm)	6.45	4.74	3.71	1.47	6.15	6.17
	Median (µm)	5.65	4.24	3.28	1.36	5.22	5.60
	Standard error (µm)	0.22	0.18	0.13	0.07	0.22	0.20
	Standard deviation	2.29	1.88	1.37	0.69	2.29	2.08
Nannoconus fragilis	Number of specimens (N)	41	41	41	41	41	41
	Minimum (µm)	2.66	2.10	1.50	0.52	2.66	2.58
	Maximum (µm)	14.05	11.07	9.05	3.32	14.05	11.2
	Mean (µm)	6.69	4.74	4.00	1.37	6.67	5.98
	Median (µm)	5.22	4.36	3.28	1.18	5.22	4.69
	Standard error (µm)	0.43	0.32	0.27	0.09	0.43	0.37
	Standard deviation	2.75	2.02	1.72	0.59	2.75	2.39
Nannoconus quadriangulus quadriangulus	Number of specimens (N)	21	21	21	21	21	21
	Minimum (µm)	4.93	2.87	1.79	1.28	4.84	4.93
	Maximum (µm)	12.70	11.49	6.52	4.33	12.66	12.7
	Mean (µm)	6.98	5.47	3.27	2.14	6.90	6.95
	Median (µm)	5.66	4.50	2.77	1.71	5.60	5.66
	Standard error (µm)	0.57	0.53	0.28	0.20	0.57	0.56
	Standard deviation	2.59	2.42	1.31	0.93	2.62	2.58
Nannoconus quadriangulus apertus	Number of specimens (N)	45	45	45	45	45	45
	Minimum (µm)	4.72	2.04	2.62	0.67	3.95	4.72
	Maximum (µm)	11.67	8.55	7.45	2.63	9.96	11.6
	Mean (µm)	5.99	4.05	3.63	1.26	5.31	5.99
	Median (µm)	5.88	3.86	3.45	1.21	4.99	5.69
	Standard error (µm)	0.20	0.16	0.14	0.06	0.18	0.20
	Standard deviation	1.35	1.11	0.92	0.39	1.19	1.35

with the size variation of the central opening and the wall thickness. In the present study, these are the elements that display the lowest degree of correlation (Figure 8).

The frequency distribution histograms and bivariate plots between the biometric parameters for all three taxa show an overlap in size distribution (Figure 5). Therefore, to confirm that the morphologic variations are independent of the size of the individuals (and thus to classify small and large specimens within the same group) we performed a Mosimann's log-shape ratio transformation (Mosimann, 1970). The size was calculated as the geometric mean of all six measurements for each specimen, and then each measurement was divided by the size to determine the shape ratio (Claude, 2013). The resulting values were used for the PCA, which shows that the first principal component explains 87.99% of the variance and is most strongly correlated with the base width, apex width, and maximum diameter (Table 4). This suggests that these components vary together. The second principal component, which explains 7.39% of variance, shows an inverse correlation between the width of the central opening and wall thickness (Table 4).

4.3. Systematic paleontology

We used the morphometric observations gathered in this study, together with the original descriptions, to clarify the distinction amongst the three taxa (Figure 9).

Nannoconus fragilis Deres & Achéritéguy, 1980

Plate 1, figs. 1–12

Description: A short cylindrical nannoconid. In longitudinal view it shows a trapezoidal shape with the length of the base slightly larger than its apical length. The central opening is U-shaped and about 2.5 to 3 times wider than the thickness of the wall. The wall is thin (1.5 to 2 µm) and sometimes striated, which gives the species a fragile appearance. The wall thins towards the opening of the apical pole, which closes by curving into the central opening. Its opposite pole is closed with rounded projections (flanges), giving the base a slightly concave shape, which is characteristic of the species (Deres & Achéritéguy, 1980).

This species is distinguished from *Nannoconus quadriangulus quadriangulus* and *N. quadriangulus apertus* by its slightly rounded basal flanges, trapezoidal-shaped test (with wide part at the base and narrow part at the apex), and a U-shaped central cavity.

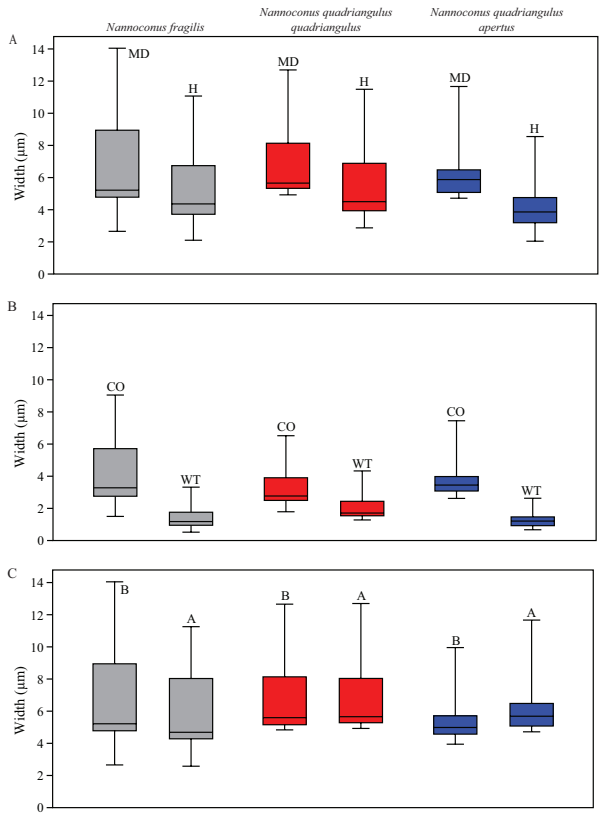

Figure 6: Box plots of **(A)** maximum diameter (MD) and height (H), **(B)** central opening (CO) and wall thickness (WT), and **(C)** base width (B) and apex width (A) of *Nannoconus fragilis* (N = 41), *N. quadriangulus quadriangulus* (N = 21), and *N. quadriangulus apertus* (N = 45).

Remarks: According to the morphometric analyses presented in this investigation, this species has characteristics similar to *N. quadriangulus apertus*, such as the differences between maximum diameter and height (MD > H), and central opening and wall thickness (CO ≥ WT). However, *N. fragilis* differs from the other studied nannoconids by having a base larger than its apex (parameter B > A). The small flanges observed at the base of the species may contribute to the width of the base always being wider than the apex. The morphometric results corroborate previous studies on the characterization of *N. fragilis*. According to Young et al. (2023), *Nannoconus fragilis* belongs to the informal group of *Nannoconus circularis* (cylindrical nannoconids with thin walls and a very wide central cavity, with the width usually at least three times the width of the walls).

Dimensions: Literature: length = 6–8 µm; width = 7–9. This study: length = 2.10–11.07 µm; width = 2.66–14.05 µm; central opening = 1.50–9.05 µm; wall thickness = 0.52–3.32 µm.

Occurrence: Restricted to the Albian (upper Subzone CC7b to lower Subzone CC9a [Sissingh, 1977] according to Perch-Nielsen, 1985). On the Brazilian continental margin, *Nannoconus fragilis* is commonly observed in association with *Prediscosphaera columnata*, *P. cretacea*, and *Axopodorhabdus albianus*, but its occurrence is confined to the interval encompassed by the planktonic foraminifera biozones *Microhedbergella renilevis* to *Ticinella primula* (Gradstein et al., 2020). This suggests that the presence of *N. fragilis* is linked to the Albian and can be correlated with lower nannofossil Zone CC8 (Sissingh, 1977; Perch-Nielsen, 1985) (Table 2).

Nannoconus quadriangulus quadriangulus Deflandre & Deflandre-Rigaud, 1962

Plate 1, figs. 13–24

Description: A short cylindrical nannoconid. Its diameter is larger than or approximately equal to its length. The diameter of the central cavity is equal to or slightly larger than the thickness of the wall, a distinctive characteristic of this species. In longitudinal view, the central opening shows a rectangular shape, similar to the outline of the test, and the walls are truncated and straight, with angular edges of thin, slightly inclined perpendicular spiral

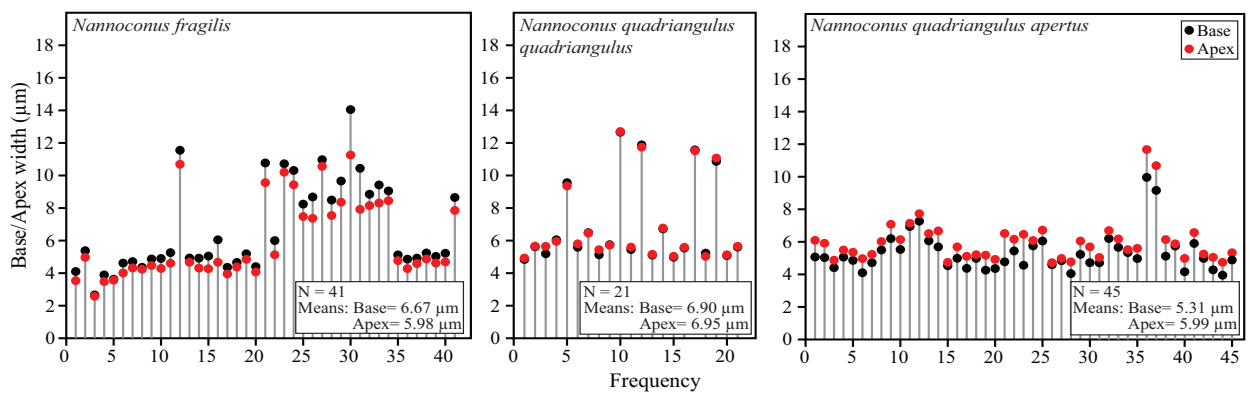

Figure 7: Frequency of base width (black) and apex width (red) of the three studied species.

Table 4: Results of the principal component analysis (PCA) for all studied morphometrics parameters. PC = principal component.

Component analyzed	PC 1	PC 2	PC 3	PC 4	PC 5	PC 6
Width of base	0.98502	0.07329	0.05082	0.10516	-0.10217	0.01694
Width of apex	0.98507	0.08910	0.03022	0.11130	0.08289	0.03913
Maximum diameter	0.98893	0.09073	0.02419	0.09649	0.02322	-0.05792
Height	0.92446	-0.03326	-0.37507	-0.059803	-0.00356	0.00186
Width of central opening	0.90936	0.35430	0.14667	-0.16128	-0.00097	0.00146
Wall thickness	0.86522	-0.48256	0.12382	-0.05651	0.00313	-0.00017
Eigenvalue	0.10287	0.00863	0.00377	0.00124	0.00030	0.00008
% variance	87.99%	7.39%	3.22%	1.06%	0.26%	0.08%

lines enclosing a well-defined apical aperture (Deflandre & Deflandre-Rigaud, 1967; Deres & Achéritéguy, 1980; Perch-Nielsen, 1985).

Remarks: The morphometric studies of *N. quadriangulus quadriangulus* confirmed unique characteristics of this subspecies when compared to other individuals under investigation. The distinctive features include the central opening and wall thickness ratio always less than 2 (CO/WT < 2), with a straight wall (between 1.28 and 4.33 µm thick) more developed than in *N. quadriangulus apertus* and a lower mean value between its maximum diameter and height. These parameters enhance the differentiation of *N. quadriangulus quadriangulus* from *N. quadriangulus apertus* and *N. fragilis*, whose central openings are more developed and walls thinner. Furthermore, our results highlight that specimens of *N. quadriangulus quadriangulus* consistently display a base approximately equal to the apex (B = A). According to Young et al. (2023), *N. quadriangulus quadriangulus* belongs to the informal group of *Nannoconus truittii*, cylindrical barrel-shaped nannoconids, with moderately wide central canals.

Dimensions: Literature: length = 5–8 µm; width = 6–10 µm; central opening = 2–3 µm. This study: length = 2.87–11.49 µm; width = 4.84–12.70 µm; central opening = 1.79–6.52 µm; wall thickness = 1.28–4.33 µm.

Occurrence: Restricted to the late Aptian, Zone CC7 of Sissingh (1977), according to Deflandre & Deflandre-Rigaud (1967), Barrier (1977), Deres & Achéritéguy (1980), Perch-Nielsen (1985), and Özkan-Altiner (1999). *Nannoconus quadriangulus quadriangulus* is found on the Brazilian continental margin often associated with *Nannoconus bucheri*, *N. circularis*, and *N. globulus*, as well as *Micrantholithus hoschulzii*. The presence of these species, along with *Eprolithus floralis*, indicate Zone CC7 (Sissingh, 1977; Perch-Nielsen, 1985). The correlation between the occurrence of *N. quadriangulus quadriangulus* and the foraminifera biozones *Globigerinelloides ferreolensis* to *Paraticinella rorhi* (Gradstein et al., 2020) in the studied sections confirms that this subspecies is restricted to the Aptian (Table 2).

Nannoconus quadriangulus apertus Deflandre & Deflandre-Rigaud, 1962

Plate 1, figs. 25–36

Description: A short and cylindrical nannoconnid related to *N. quadriangulus quadriangulus*. However, it differs from the latter based on the gradual separation between its walls from the basal to apical apertures. Its central cavity is slightly wider than in *N. quadriangulus quadriangulus* with a trapezoidal shape (with a narrow part at the base

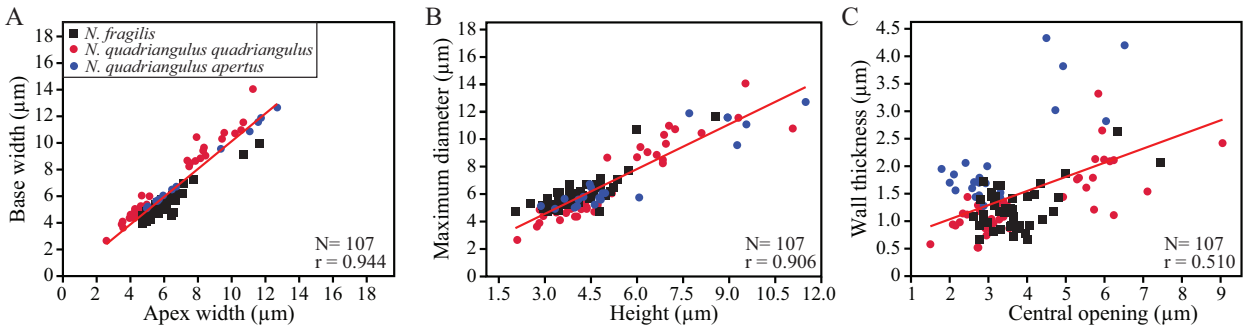

Figure 8: Cross plots of **(A)** apex width versus base width, **(B)** height versus maximum diameter, and **(C)** central opening versus wall thickness for all measured specimens (N = 107) of *Nannoconus fragilis*, *N. quadriangulus quadriangulus*, and *N. quadriangulus apertus*. Pearson's correlation coefficient (r) and the linear regression line are shown for each plot. Probabilities p < 0.0001.

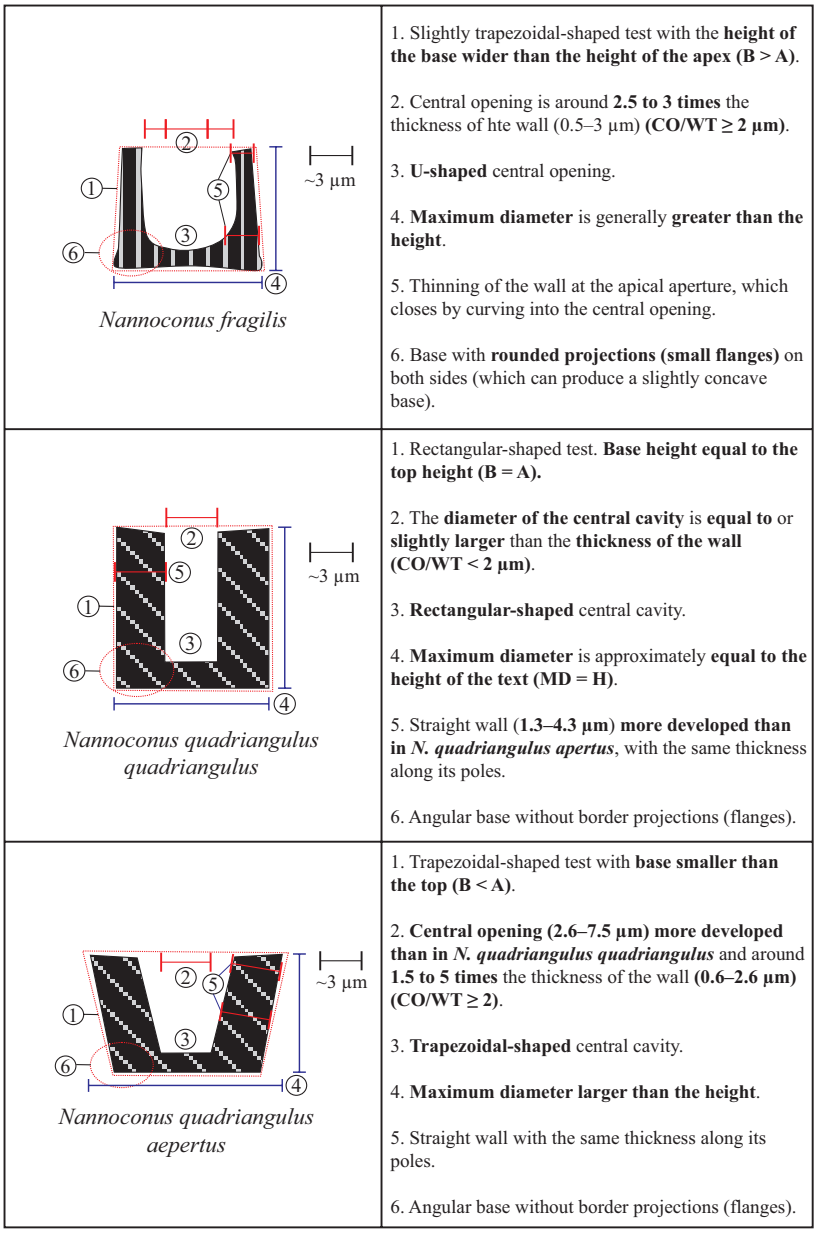

Figure 9: Proposed morphometric diagnoses of *Nannoconus fragilis*, *N. quadriangulus quadriangulus*, and *N. quadriangulus apertus* based on this morphometric study. A = apex, B = base, CO = central opening, WT = wall thickness, MD = maximum diameter, H = height.

and wide part at the apex), similar to the outline of the test. For this reason, *N. quadriangulus apertus* commonly exhibits larger dimensions than *N. quadriangulus quadriangulus.*

Remarks: The morphometric results presented in this study corroborate previous studies and refine the diagnostic characteristics of the subspecies. When compared to *N. fragilis* and *N. quadriangulus quadriangulus*, *N. quadriangulus apertus* exhibits a larger average size, but is closer in size to *N. fragilis*. It features a more developed central opening and thinner walls compared to *N. quadriangulus quadriangulus*, along with a base that is narrower than its apex (B < A). According to Young et al. (2023), *N. quadriangulus apertus* belongs to the informal group of *Nannoconus truittii*.

Dimensions: Literature: length = 5–8 µm; width = 5.5–11 µm; central opening = 3–5 µm. This study: length = 2.04–8.55 µm; width = 3.95–11.67 µm; central opening = 2.62–7.45 µm; wall thickness = 0.67–2.63 µm.

Occurrence: Restricted to the late Aptian, Zone CC7 of Sissingh (1977), according to Deflandre & Deflandre-Rigaud (1967), Barrier (1977), Deres & Achéritéguy (1980), Perch-Nielsen (1985), and Özkan-Altiner (1999). In Brazil, the geological range of *N. quadriangulus apertus* is the same as that of *N. quadriangulus quadriangulus*, which is described as restricted to the Aptian.

5. Discussion and conclusions

This study used samples from 38 wells on the Brazilian continental margin to characterize the morphology of *Nannoconus fragilis*, *N. quadriangulus quadriangulus*, and *N. quadriangulus apertus*. The synthesis of biostratigraphic and bibliographic research and the morphometric data provide a significant improvement to the taxonomic differentiation based on the base/apex, the maximum diameter/height, and the central opening/wall thickness. Statistical methods indicate that the central opening/wall thickness has low correlation and therefore may be strongly influenced by diagenetic alteration. This morphometric study shows a clear correlation with the descriptions of the holotypes of the taxa investigated, but also clarifies problematic questions about the identification of *N. fragilis* and the *N. quadriangulus* group (Figure 9).

Our study confirmed the biostratigraphic observations of most previous studies in other areas of the world as well as those conducted on the Brazilian continental margin. We found that the occurrences of *N. quadriangulus quadriangulus* and *N. quadriangulus apertus* are restricted to the Aptian, which is suggested by their presence in the foraminiferal biozones *Globigerinelloides ferreolensis – Paraticinella rorhi*, which are correlated to Subzone CC7b (Sissingh, 1977; Perch-Nielsen, 1985). Moreover, the presence of *N. fragilis* is limited to the Albian. It is consistently found in association within the interval of foraminiferal biozones *Microhedbergella renilevis* to *Ticinella primula*, correlating to lower Zone CC8 (Sissingh, 1977; Perch-Nielsen, 1985). Previous inconsistencies in the biostratigraphic interpretations of *N. fragilis*, *N. quadriangulus quadriangulus*, and *N. quadriangulus apertus* likely derived from their high morphological variability in combination with poor preservation. Once the proposed revised taxonomy is applied, further studies of potential paleoenvironmental constraints and paleoecological affinities might reveal differential distribution in space and time.

Acknowledgements

The authors would like to thank José Ricardo Maizatto, Christiano Ng, and Elizabete Pedrão Ferreira (PETROBRAS/CENPES) for their advice and comments. The authors would also like to thank the editor, Denise Kulhanek, for her constructive comments, patience, and assistance, and the reviewers (Elisabetta Erba and Juan Pablo Pérez Panera) for their valuable comments, which helped to improve the manuscript.

Funding

This research did not receive any specific grant from funding agencies in the public, commercial, or nonprofit sectors.

References

Aarhus, N., Verdenius, J. & Birkelund, T. 1986. Biostratigraphy of a Lower Cretaceous section from Sklinnabanken, Norway, with some comments on the Andoya exposure. *Norsk Geologisk Tidsskrift*, **66**: 17–43.

Aguirre-Urreta, B., Schmitz, M., Lescano, M., Tunik, M., Rawson, P., Concheyro, A., Buhler, M. & Ramos, V. 2017. A high precision U-Pb radioisotopic age for the Agrio Formation, Neuquén Basin, Argentina: Implications for the chronology of the Hauterivian Stage. *Cretaceous Research*, **75**: 193–204. https://doi.org/10.1016/j.cretres.2017.03.027

Aguirre-Urreta, B., Martinez, M., Schmitz, M., Lescano, M., Omarini, J., Tunik, M., Kuhnert, H., Concheyro, A., Rawson, P., Ramos, V., Reboulet, S., Noclin, N., Frederichs, T., Nickl, A. & Pälike, H. 2019. Interhemispheric radio-astrochronological calibration of the time scales from the Andean and the Tethyan areas in the Valanginian–Hauterivian (Early Cretaceous). *Gondwana Research*, **70**: 104–132. https://doi.org/10.1016/j.gr.2019.01.006

Al-Fares, A.A., Bouman, M. & Jeans, P. 1998. A new look at the middle to Lower Cretaceous stratigraphy, offshore Kuwait. *Geoarabia*, **3**(4): 543–560. https://doi.org/10.2113/geoarabia0304543

Al-Miamary, F.A., Al-Badrani, O.A., & Al-Juboury, A.I. 2020. Calcareous nannofossils and chemostratigraphy of the early Aptian oceanic anoxic event 1a from Northern Iraq. *Bulletin of the Iraq Natural History Museum*, **16**(1): 95–111. https://doi.org/10.26842/binhm.7.2020.16.1.0095

Alves, C.F., Lima, F.H. de O. & Shimabukuro, S. 2017. New Aptian calcareous nannofossil species from Brazil. *Journal of Nannoplankton Research*, **37**(1): 15–24. https://doi.org/10.58998/jnr2004

Antunes, R.L. 1996. Biozonas de nanofósseis do Cretáceo da margem continental Brasileira: problemas e possíveis soluções. *Boletim de Geociências da PETROBRAS*, **10**(1/4): 19–42.

Antunes, R.L. 1998. *Nanofósseis calcários e sua bioestratigrafia no Cretáceo da margem continental brasileira: Bacias*

do Ceará e Potiguar. Unpublished PhD Thesis. Universidade Federal do Rio de Janeiro, Rio de Janeiro: 193pp.

Aubry, M.P. 1974. Remarques sur la systématique des Nannoconus de la Craie. *Cahiers de Micropaléontologie*, **4**: 3–22.

Baldi-Beke, M. 1962. A Magyarországi Nannoconuszok (Protozoa inc. sedis). *Geologica Hungarica series Palaeontologica*, **30**: 109–148.

Banner, F.T. & Desai, D. 1988. A review and revision of the Jurassic–Early Cretaceous Globigerinina, with special reference to the Aptian assemblages of Speeton (North Yorkshire, England). *Journal of Micropalaeontology*, **7**(2): 143–185.

Barbarin, N., Bonin, A., Mattioli, E., Pucéat, E., Cappetta, H., Gréselle, B., Pittet, B., Vennin, E. & Joachimski, M. 2012. Evidence for a complex Valanginian nannoconid decline in the Vocontian Basin (South East France). *Marine Micropaleontology*, **84–85**: 37–53. https://doi.org/10.1016/j.marmicro.2011.11.005

Barrier, J. 1977. Nannofossiles calcaires du Gargasien stratotypique. *Bulletin du Museum National D'Histoire Naturelle, Sciences de la Terre*, **62**(485): 173–227.

Bornemann, A., Aschwer, U. & Mutterlose, J. 2003. The impact of calcareous nannofossils on the pelagic carbonate accumulation across the Jurassic–Cretaceous boundary. *Palaeogeography, Palaeoclimatology, Palaeoecology,* **199**: 187–228. https://doi.org/10.1016/S0031-0182(03)00507-8

Bornemann, A., Pross, J., Reichelt, K., Herrle, J.O., Hemleben, C. & Mutterlose, J. 2005. Reconstruction of short-term palaeoceanographic changes during the formation of the Late Albian "Niveau Breistroffer" black shales (Oceanic Anoxic Event 1d, SE France). *Journal of the Geological Society*, **162**(4); 623–639. https://doi.org/10.1144/0016-764903-171

Bouché, P.M. 1963. Etat des connaissances sur les nannofossiles calcaires du Crétacé Inferieur. *Memoires du Bureau de Recherches Géologiques et Minières*, **34**: 451–459.

Bouché, P.M. 1965. Eléments pour une définition d'un stratotype du Barrémien. III. Nannofossiles calcaires. *Memoires du Bureau de Recherches Géologiques et Minières*, **34**: 131–138.

Bown, P.R. (Ed.) 1998. *Calcareous Nannofossil Biostratigraphy*. British Micropaleontological Society Publications Series. Chapman & Hall, London: 315pp.

Bown, P.R. & Concheyro, A. 2004. Lower Cretaceous calcareous nannoplankton from the Neuquen Basin, Argentina. *Marine Micropaleontology*, **52**(1–4): 51–84. https://doi.org/10.1016/j.marmicro.2004.04.006

Bown P.R. & Young J.R. 1998. Techniques. *In*: P.R. Bown (Ed.) *Calcareous Nannofossil Biostratigraphy*. British Micropalaeontology Society Publication Series. Chapman & Hall, London: 16–28.

Bralower, T., Monechi, S. & Thierstein, H. 1989. Calcareous nannofossil zonation of the Jurassic–Cretaceous boundary interval and correlation with the geomagnetic polarity timescale. *Marine Micropaleontology*, **14**(1–3): 153–235. https://doi.org/10.1016/0377-8398(89)90035-2

Brönnimann, P. 1955. Microfossils incertae sedis from the Upper Jurassic and Lower Cretaceous of Cuba. *Micropaleontology*, **1**: 28–51.

Casellato, C.E. 2010. Calcareous nannofossil biostratigraphy of Upper Callovian–Lower Berriasian successions from the Southern Alps, North Italy. *Rivista Italiana Paleontologie e Stratigrafia*, **116**: 357–404. https://doi.org/10.13130/2039-4942/6394

Cassab, R.C.T., Santos, E.C.M, Fernandes, A.C.S., Brito, I.M., Ismar, S.C., Coimbra, J.C., Moura, J.A., Duarte, L., Freitas, L.C., Hessel, M.H.R., Carvalho, M.S.S., Viviers, M.C. & Uesugui, N. 1994. The Sergipe-Alagoas Basin. *In*: G. Beurlen, D.A. Campos, M.C. Viviers (Eds.). *Stratigraphic Range of Cretaceous Mega- and Microfossils of Brazil.* Universidade Federal do Rio de Janeiro: 161–231.

Claude, J. 2013. Log-shape ratios, Procrustes superimposition, elliptic Fourier analysis: three worked examples in *R. Hystrix-italian. Journal of Mammalogy*, **24**: 94–102. https://doi.org/ doi:10.4404/hystrix-24.1-6316

Colom, G. 1945. *Nannoconus steinmanni* Kamptner y Lagena colomi Lapparent. *Publication Institute Geologicas Provincio Barcelona, Miscelldnea Aimera*, **7**(1): 123–132.

Concheyro, A. & Sagasti, G. 1999. Lower Cretaceous calcareous nannofossils of Agrio Formation, Mendoza Province, Argentina. *Boletim do 5 Simposio sobre o Cretáceo do Brasil.* UNESP. Campus de Rio Claro/SP: 359–365.

Concheyro, A., Lescano, M., Caramés, A. & Ballent, S. 2009. Micropaleontología de la Formación Agrio (Cretácico Inferior) en distintos sectores de la Cuenca Neuquina. *Revista de la Asociación Geológica Argentina*, **65**(2): 342–361.

Cunha, A.A.S. 1990a. *Bioestratigrafia dos nanofósseis calcários da Sub-bacia de Mundaú (Bacia do Ceará).* Unpublished Master Thesis. Universidade Federal do Rio Grande do Sul, Porto Alegre: 151pp.

Cunha, A.A.S. 1990b. *Nannoconus fragilis e Braarudosphaera africana*: Duas novas biozonas de Nanofósseis calcários da Bacia do Ceará, Brasil. *Boletim de Geociências da PETRO-*

BRAS, **4**(3): 275–284.

Cunha, A.A.S. & Koutsoukos, E.A.M. 1998. Calcareous nannofossils and planktic foraminifers in the upper Aptian of the Sergipe Basin, northeastern Brazil: palaeoecological inferences. *Palaeogeography, Palaeoclimatology, Palaeoecology*, **142**(3–4): 175–184. https://doi.org/10.1016/S0031-0182(98)00065-0

Cunha, A.A.S. & Shimabukuro, S. 1997. *Braarudosphaera* blooms and anomalous enrichments of *Nannoconus*: evidence from the Turonian South Atlantic, Santos Basin, Brazil. *Journal of Nannoplankton Research*, **19**(1): 51–55. https://doi.org/10.58998/jnr2217

de Lapparent, J. 1925. Sur une variété de calcaire à grain fin. *Comptes Rendus Sommaire des Séances de la Societé Géologique de France*, **7**: 104–106.

Deflandre, G. & Deflandre-Rigaud, M. 1962. Remarques sur l'évolution des Nannoconidés à propos de quelques nouveaux types du Crétacé inferieur de Haute-Provence. *Comptes Rendus de L'Academie des Sciences*, **255**: 2638–2640.

Deflandre, G. & Deflandre-Rigaud, M. 1967. Diagnoses de quelques nouveaux Nannoconidées gargasiens de Haute Provence. *Bulletin du Museum National D'Histoire Naturelle*, **2**(39): 774–778.

Deres, F. & Achéritéguy, J. 1972. Contribution à etude des nannoconidés dans le Crétacé Inferieur Du Bassin d'Aquitaine. *Memoires du Bureau de Recherches Géologiques et Minières*, **77**: 153–163.

Deres, F. & Achéritéguy, J. 1980. Biostratigraphie des Nannoconides. *Bulletin des Centres de Recherches Exploration-Production Elf-Aquitaine*, **4**: 1–53.

Farinacci, A. 1969 (et seq.). *Catalogue of Calcareous Nannofossils*. Edizioni Tecnoscienza, Roma.

Freitas, L.C.S., Antunes, R.L., Shimabukuro, S., Richter, A.J. & Gomide, J. 1986. Sergipe-Alagoas Basin — A reconnaissance of Aptian/Early Albian marine-sediments based upon calcareous nannoplankton. *Anais da Academia Brasileira de Ciências*, **58**(4): 613.

Gale, A.S., Bown, P., Caron, M., Crampton, J., Crowhurst, S.J., Kennedy, W.J., Petrizzo, M.R. & Wray, D.S. 2011. The uppermost Middle and Upper Albian succession at the Col de Palluel, Hautes-Alpes, France: An integrated study (ammonites, inoceramid bivalves, planktonic foraminifera, nannofossils, geochemistry, stable oxygen and carbon isotopes, cyclostratigraphy). *Cretaceous Research*, **32**(2): 59–130. https://doi.org/10.1016/j.cretres.2010.10.004

Gombos, A.M., Strohmenger, C.J. & Huang, T.C. 2007. Biostratigraphic constraints on the Shuaiba Formation, Abu Dhabi, United Arab Emirates. International Petroleum Technology Conference (ITPC), Dubai, United Arab Emirates, paper number IPTC-11206-MS. https://doi.org/10.2523/IPTC-11206-MS

Gradstein, F., Ogg, J.G., Schmitz, M.D. & Ogg, G.M. 2020. *Geologic Time Scale 2020*. Elsevier, Amsterdam: 1357pp.

Hassanein, W. 2016. The Late Aptian–Albian Transgression in the Agadir-Essaouira Basin, Morocco. Applied Geology. Unpublished PhD Thesis. Université Grenoble Alpes; Ǧāmiʿaï al-Qāhiraï: 309pp.

Hernández, Y. 2012. *Estratigrafía del área Rio Frío-Cerro Las Minas, estado Táchira Venezuela*. Unpublished Master Thesis. Universidad Central de Venezuela: 127pp.

Herrle, J.O. 2003. Reconstructing nutricline dynamics of mid-Cretaceous oceans: evidence from calcareous nannofossils from the Niveau Paquier black shale (SE France). *Marine Micropaleontology*, **47**(3–4): 307–321. https://doi.org/10.1016/S0377-8398(02)00133-0

Herrle, J.O. & Mutterlose, J. 2003. Calcareous nannofossils from the Aptian-Lower Albian of southeast France: palaeoecological and biostratigraphic implications. *Cretaceous Research*, **24**(1): 1–22. https://doi.org/10.1016/S0195-6671(03)00023-5

Hippolyte, J.C., Müller, C., Kaymakci, N. & Sangu, E. 2010. Dating of the Black Sea Basin: New nannoplankton ages from its inverted margin in the Central Pontides (Turkey). *In*: M. Sosson, N. Kaymakçi, R.A. Stephenson, F. Bergerat & V. Starostenko (Eds.). *Sedimentary Basin Tectonics from the Black Sea and Caucasus to the Arabian Platform*. Geological Society of London, Special Publication, **340**: 113–136. https://doi.org/10.1144/SP340.7

Jeremiah, J.M. 2001. A Lower Cretaceous nannofossil zonation for the North Sea Basin. *Journal of Micropalaeontology*, **20**: 45–80. https://doi.org/10.1144/jm.20.1.45

Kamptner, E. 1931. *Nannoconus steinmanni* nov. gen., nov. spec., ein merkwürdiges gesteinsbildendes Mikrofossil aus dem jüngeren Mesozoikum der Alpen. *Paläontologische Zeitschrift*, **13**: 288–297. https://doi.org/10.1007/BF03044000

Kamptner, E. 1938. Einige Bemerkungen über *Nannoconus*. *Paläontologische Zeitschrift*, **20**: 249–257. https://doi.org/10.1007/BF03041919

Kaiser-Weidich, B. & Schairer, G. 1990. Stratigraphische Korrelation von Ammoniten, Calpionellen und Nannoconiden

aus Oberjura und Unterkreide der Nördlichen Kalkalpen. *Eclogae Geologicae Helvetiae*, **83**(2): 353–387.

Kennedy, W.J., Gale, A.S., Bown, P.R., Caron, M., Davey, R.J., Gröcke, D. & Wray, D.S. 2000. Integrated stratigraphy across the Aptian–Albian boundary in the Marnes Bleues, at the Col de Pré-Guittard, Arnayon (Drôme), and at Tartonne (Alpes-de-Haute-Provence), France: a candidate Global Boundary Stratotype Section and Boundary Point for the base of the Albian Stage. *Cretaceous Research*, **21**(5): 591–720. https://doi.org/10.1006/cres.2000.0223

Khodadadi, L. & Hadavi, F. 2013. Nannostratigraphy and palaeoecology of Tirgan and Sarcheshmeh Formations in Taherabad and Mozduran section. *Sedimentary Facies*, **5**(2): 196–210. https://doi.org/10.22067/SED.FACIES.V5I2.10513

Lambert, B.C. 2022. Calcareous nannofossils of the uppermost Bedoulian and lower Gargasian of La Tuilière – St-Saturnin-lès-Apt (area of the Aptian stratotype, Vaucluse, SE France). *Carnets de Geologie*, **22**(17): 745–793. https://doi.org/10.2110/carnets.2022.2217

Lambert, B. & Laporte-Galaa, C. 1996. Nannoflore calcarie du puits Mango 1 (Offshore nord Sinai, Égypte). *Bulletin des Centres de recherches exploration-production Elf-Aquitane. Memoire*, **16**: 631–645.

Lescano, M. & Concheyro, A. 2014. Nanocónidos del Grupo Mendoza (Cretácico Inferior) en la Provincia del Neuquén, República Argentina: taxonomía, cronoestratigrafía e implicancias paleogeográficas. *Ameghiniana*, **51**(6): 466–499. https://doi.org/10.5710/AMGH.06.08.2014.1838

Lima, F.H.O., Sanjinés, A.E.S., Maizatto, J.R., Ferreira, E.P., Ng, C., Costa, D.S., Zerfass, G.S.A., Alves, C.F., Strohschoen Jr., O., Viviers, M.C., Lana, C.C., Arai, M., Beurlen, G., Shimabukuro, S. & Galm, P.C. 2018. Aptian marine post-salt rocks in Santos, Campos and Espírito Santo basins, Brazil: a biochronostratigraphical approach. *Anais do 49° Congresso Brasileiro de Geologia* (abstract). http://cbg2018anais.siteoficial.ws/resumos/4924.pdf

Lima, F.H.O., Sanjinés, A.E.S., Maizatto, J.R., Ferreira, E.P., Ng, C., Costa, D.S., Zerfass, G.S.A., Alves, C.F., Strohschoen Jr., O., Viviers, M.C., Lana, C.C., Arai, M., Beurlen, G. & Shimabukuro, S. 2019. Aptian age to post-salt section in Brazilian southeastern coastal basins: new biochronostratigraphic insights about South Atlantic evolution. *3rd International Congress on Stratigraphy* (abstract), Italy, p. 393.

Longoria, J.F. 1977. Biostratigrafía del Cretácico Inferior basada en microfósiles planctónicos. *Boletín de la Sociedad Geológica Mexicana*, **38**(1): 2–17. https://doi.org/10.18268/BSGM1977v38n1a1

Longoria, J.F. 1984. Cretaceous biochronology from the Gulf of Mexico region based on planktonic microfossils. *Micropaleontology*, **30**(3): 225–242. https://doi.org/10.2307/1485687

Mahanipour, A., Mutterlose, J., Kani, A.L. & Adabi, M.H. 2011. Palaeoecology and biostratigraphy of early Cretaceous (Aptian) calcareous nannofossils and the $\delta^{13}C_{carb}$ isotope record from NE Iran. *Cretaceous Research*, **32**(3): 331–356. https://doi.org/10.1016/j.cretres.2011.01.006

Manivit, H. 1971. *Nannofossiles calcaires du Crétacé francais (Aptien-Maestrichtien). Essai de Biozonation appuyée sur les stratotypes*. Unpublished PhD Thesis. Université de Paris: 187pp.

Milani, E.J. (Coord.), Rangel, H.D., Bueno, G.V., Stica, J.M., Winter, W.R., Caixeta, J.M. & Pessoa Neto, O.C. 2007. Bacias Sedimentares Brasileiras — cartas estratigráficas. *Boletim de Geociências da PETROBRAS*, Rio de Janeiro, Brazil, **15**(2): 183–573.

Moshkovitz, S. 1972. Biostratigraphy of the genus *Nannoconus* in the Lower Cretaceous sediments of the subsurface: Ashqelon-Helez area, Central Israel. *Israel Journal of Earth Sciences*, **21**: 1–28.

Mosimann, J.E. 1970. Size allometry: size and shape variables with characterizations of the lognormal and generalized gamma distributions. *Journal of the American Statistical Association*, **65**: 930–948. https://doi.org/10.1080/01621459.1970.10481136

Noël, D. 1958. Étude de coccolithes du Jurassique et du Crétacé inférieur. *Publications du Service de la Carte Géologique de l'Algérie (Nouvelle Serie)*, **2**(20): 155–196.

Noël, D. 1965. Sur les Coccolithes du Jurassique Européen et d'Afrique du Nord. Essai de classification des coccolithes fossiles. *Éditions du Centre National de la Recherche Scientifique*, Paris: 209pp.

Özkan-Altiner, S. 1996. Calcareous nannofossil biostratigraphy of Valanginian-Aptian in Northwest Anatolia, Turkey. *Revue de Paléobiologie*, **15**(2): 479–498.

Özkan-Altiner, S. 1999. Rock-forming nannofossils in uppermost Jurassic–Lower Cretaceous rock units of Northwest Anatolia: *Nannoconus* and its revised taxonomy. *Turkish Journal of Earth Sciences*, **8**(1): 19–43.

Pedrosa, F.A. 2013. *Estudo bioestratigráfico com base em nanofósseis calcários do Cretáceo da Bacia de Sergipe, Nordeste do Brasil*. Unpublished Master Thesis. Universidade Federal de Pernambuco, Recife: 165pp.

Pedrosa, F.A., Araújo, I.G., Antunes, R.L. & Lima-Filho, M.F.

2019. Estudo Bioestratigráfico com Base em Nanofósseis Calcários do Cretáceo da Bacia de Sergipe, Nordeste do Brasil. *Anuário do Instituto de Geociências*, **42**(3): 207–222. https://doi.org/10.11137/2019_3_207_222

Perch-Nielsen, K. 1985. Mesozoic calcareous nannofossils. *In*: H.M. Bolli, J.B. Saunders & K. Perch-Nielsen (Eds.). *Plankton Stratigraphy*. Cambridge University Press, Cambridge: 329–426.

Pszczółkowski, A. 2015a. Aptian age of the "spotted limestone" (Pieniny Limestone Formation) in Grajcarek Stream (Pieniny Klippen Belt, Poland). *Annales Societatis Geologorum Poloniae*, **85**: 21–42. https://doi.org/10.14241/asgp.2014.001

Pszczółkowski, A. 2015b. Aptian foraminiferal stratigraphy and *Nannoconus* assemblage Kopka Section (Western Tatra Mountains, Poland). *Annales Societatis Geologorum Poloniae*, **85**: 123–138. https://doi.org/10.14241/asgp.2014.004

Robert, A.M.M., Letouzey, J., Kavoosi, M.A., Sherkati, S., Müller, C., Vergés, J. & Aghababaei, A. 2014. Structural evolution of the Kopeh Dagh fold-and-thrust belt (NE Iran) and interactions with the South Caspian Sea Basin and Amu Darya Basin. *Marine and Petroleum Geology*, **57**: 68–87. https://doi.org/10.1016/j.marpetgeo.2014.05.002

Romey, C., Rochette, P., Vella, C., Arfib, B., Andrieu-Ponel, V., Braucher, R., Champollion, C., Douchet, M., Dussouillez, P., Hermitte, D., Mattioli, E., Parisot, J.-C. & Schwenninger, J.-L. 2014. Geophysical and geomorphological investigations of a Quaternary karstic paleolake and its underground marine connection in Cassis (Bestouan, Cassis, SE France). *Geomorphology*, **214**: 402–415. https://doi.org/10.1016/j.geomorph.2014.02.021

Rutledge, D.C. 1994. *Calcareous nannofossils of the Boreal Lower Cretaceous: applications in biostratigraphy and palaeoceanography*. Unpublished PhD Thesis. University College London: 324pp.

Sanjinés, A.E.S., Viviers, M.C., Costa, D.S., Zerfass, G.S.A., Johnsson, C.C., Strohschoen Jr., O., Beurlen, G. & Lima, F.H.O. 2019. Earlier South Atlantic marine ingression in brazilian Southeastern basins, based on Aptian planktonic foraminifera evidences. *3rd International Congress on Stratigraphy* (abstract), Italy, p. 394.

Sanjinés, A.E., Viviers, M.C., Costa, D.S., de Santana dos Anjos Zerfass, G., Beurlen, G. & Strohschoen, O. 2022. Planktonic foraminifera from the Aptian section of the southeastern Brazilian Atlantic Margin. *Cretaceous Research*, **134**: 105141. https://doi.org/10.1016/j.cretres.2022.105141

Silva, R., de Moraes Rios-Netto, A., Silva, S., Valle, B., Borghi, L. & Abbots-Queiroz, F. 2020. Middle Cretaceous calcareous nannofossils from the cored well UFRJ-2-LRJ-01-SE, Sergipe-Alagoas Basin, Brazil: New biostratigraphy and paleobiogeographic inferences. *Cretaceous Research*, **106**: 104245. https://doi.org/10.1016/j.cretres.2019.104245

Sissingh, W. 1977. Biostratigraphy of Cretaceous calcareous nannoplankton. *Geologie Mijinbouw*, **56**: 37–65.

Thierstein, H.R. 1973. Lower Cretaceous calcareous nannoplankton biostratigraphy. *Abhandlungen der Geologischen Bundesanstalt*, **29**: 1–52.

Trejo, H.M. 1960. La familia Nannoconidae y su alcance estratigráfico en América. *Boletín de la Asociación Mexicana de Geólogos Petroleros*, **12**: 259–314.

Tremolada, F. & Young, J.R. 2002. Volume calculation of Cretaceous calcareous nannofossils. *Journal of Nannoplankton Research*, **24**: 199–202. https://doi.org/10.58998/jnr2244

Troelsen, J.C. & Quadros, L.P. 1971. Distribuição bioestratigráfica dos nanofósseis em sedimentos marinhos (Aptiano-Mioceno) do Brasil. *Anais Academia Brasileira de Ciências*, **43**: 577–609.

van Buchem, F.S.P., Simmons, M.D., Droste, H.J. & Davies, R.B. 2011. Late Aptian to Turonian stratigraphy of the eastern Arabian Plate — depositional sequences and lithostratigraphic nomenclature. *Petroleum Geoscience*, **17**(3): 211–222. https://doi.org/10.1144/1354-079310-061

van Niel, B.E. 1992. New observations on the morphology of Nannoconus. *In*: B. Hamrsmid & J.R. Young (Eds.). Proceedings of the Fourth INA Conference, Prague 1991, *Nannoplankton Research*, **1**: 73–85.

van Niel, B.E. 1994. A review of the terminology used to describe the genus *Nannoconus* (calcareous nannofossil, incertae sedis). *Cahiers de Micropaléontotologie*, **9**: 27–47.

Verdenius, J.G. 1993. Late Cretaceous calcareous nannoplankton zonation of Jamaica. *Geological Society of America Memoirs*, **182**: 1–18. https://doi.org/10.1130/MEM182-p1

Viviers, M.C., Sanjinés, A.E.S., Costa, D.S., Zerfass, G.S.A., Beurlen, G. & Stroschoen Jr., O. 2018. Aptian planktonic foraminifera occurrence in the southeastern Brazilian marginal basins. *Anais do 49° Congresso Brasileiro de Geologia* (abstract). http://cbg2018anais.siteoficial.ws/resumos/7442.pdf

Watkins, D.K. & Bowdler, J.L. 1984. Cretaceous calcareous nannofossils from Deep Sea Drilling Project Leg 77, southeast Gulf of Mexico. *Initial Reports of the Deep-Sea Drilling Project*, **77**: 649–674. https://doi.org/10.2973/dsdp.

proc.77.127.1984

Watkins, D.K., Cooper, M.J. & Wilson, P.A. 2005. Calcareous Nannoplankton response to late Albian Oceanic Anoxic Event 1d in the Western North Atlantic. *Paleoceanography*, **20**: 1–14. https://doi.org/10.1029/2004PA001097

Watkins, D.K. & Verbeek, J.W. 1988. Calcareous nannofossil biostratigraphy from Leg 101, Northern Bahamas. *Proceedings of the Ocean Drilling Program*, *Scientific Results*, **101**: 3–86. https://doi.org/10.2973/odp.proc.sr.101.131.1988

Witt, W. & Gökdag, H. 1994. Orbitolinid biostratigraphy of the Shu'aiba Formation (Aptian), Oman - implications for reservoir development. *In*: M.D. Simmons (Ed.). *Micropalaeontology and Hydrocarbon Exploration in the Middle East*. Chapman and Hall, London: 221–242.

Wiegand, G.E. 1984. Nannofossils from the Northwest African Margin, Deep Sea Drilling Project Leg 79. *Initial Reports of the Deep Sea Drilling Project*, **79**: 567–578. https://doi.org/10.2973/dsdp.proc.79.121.1984

Young, J.R., Bergen, J.A., Bown, P.R., Burnett, J.A., Fiorentino, A., Jordan, R.W., Kleijne, A., van Niel, B.E., Romein, A.J.T. & von Salis, K. 1997. Guidelines for coccolith and calcareous nannofossil terminology. *Palaeontology*, **40**(4): 875–912.

Young, J.R., Bown, P.R. & Lees J.A. 2023. *Nannotax3 website*. International Nannoplankton Association. Accessed 29 May 2023. URL: https://www.mikrotax.org/Nannotax3

Youssef, A.H. & Kadar, A.P. 2012. Sequence stratigraphy framework of late Albian to early Cenomanian Wara and Ahmadi Formations, onshore Kuwait. *Middle East Geosciences Conference and Exhibition*, **10**. https://doi.org/10.3997/2214-4609-pdb.287.1218261

Youssef, A.H., Al-Sahlan, G., Karam, K.A., Packer, S., Starkie, S. & Stead, D. 2019. Sequence stratigraphic framework of the Wara and Ahmadi formations, onshore Kuwait: *Stratigraphy*, **16**(1): 1–26. https://doi.org/10.29041/strat.16.1.1-26

Plate 1

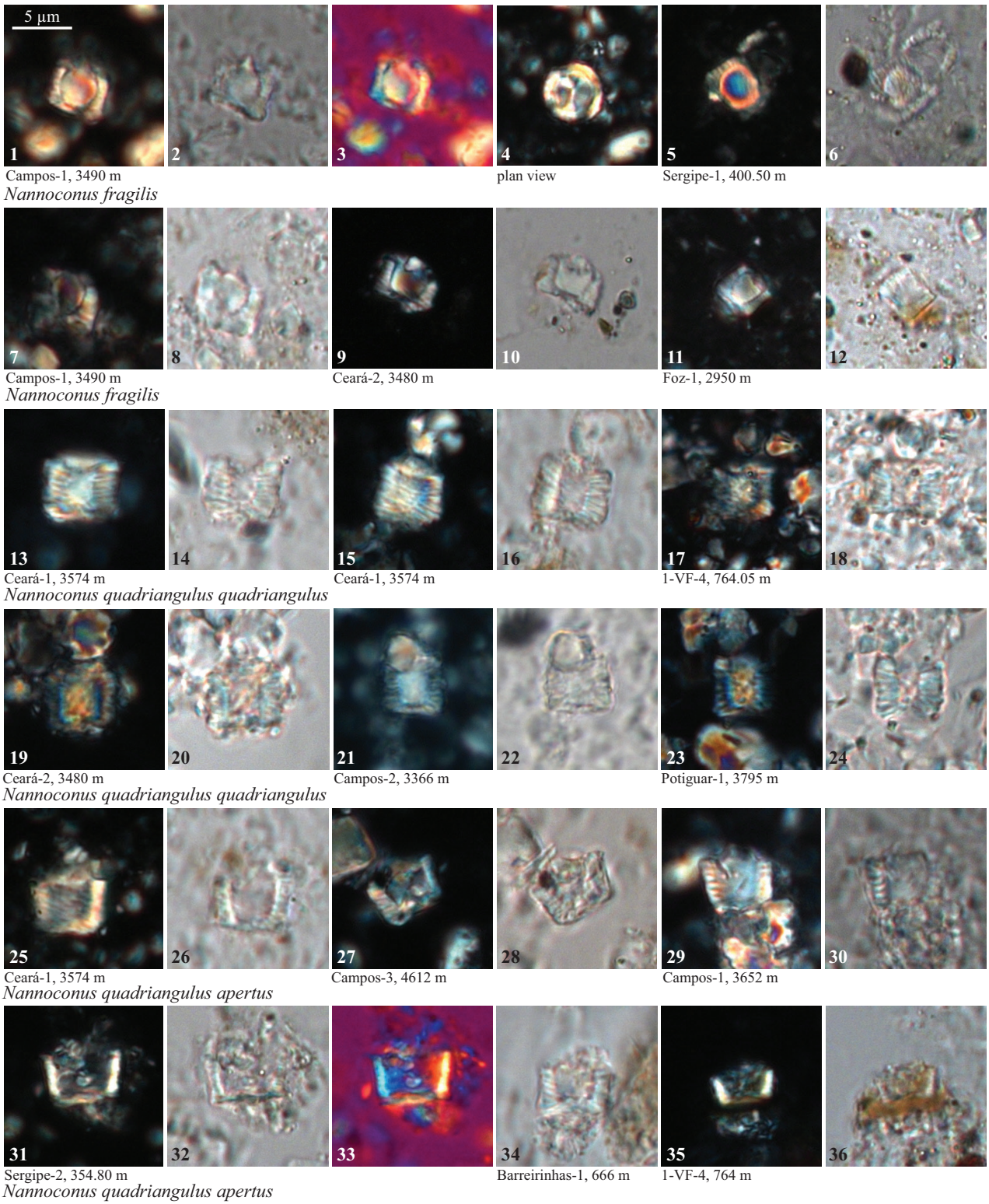

Plate 1: Photomicrographs of *Nannoconus* specimens from the Brazilian continental margin. Images with a black background taken under cross-polarized light, a grey background under brightfield, and a pink background with a gypsum plate.

	Nannoconus fragilis						*Nannoconus quadriangulus quadriangulus*						*Nannoconus quadriangulus apertus*					
Specimen	Base Width (B)	Apex Width (A)	Maximum Diameter (MD)	Height (H)	Central Opening (CO)	Maximum Wall Thickness (WT)	Base Width (B)	Apex Width (A)	Maximum Diameter (MD)	Height (H)	Central Opening (CO)	Maximum Wall Thickness (WT)	Base Width (B)	Apex Width (A)	Maximum Diameter (MD)	Height (H)	Central Opening (CO)	Maximum Wall Thickness (WT)
1	4.10	3.54	4.10	3.49	2.15	0.92	4.84	4.93	4.93	3.33	2.67	1.44	5.07	6.09	6.09	4.11	4.05	0.92
2	5.38	4.97	5.38	4.31	3.28	1.03	5.62	5.66	5.66	4.80	2.76	1.47	5.03	5.91	5.91	4.98	3.56	1.23
3	2.66	2.58	2.66	2.10	1.50	0.58	5.19	5.65	5.65	3.90	3.31	1.52	4.41	4.87	4.87	3.18	2.87	1.13
4	3.89	3.48	3.89	2.82	2.08	0.94	6.05	5.95	6.05	4.87	2.97	2.00	5.06	5.50	5.50	3.80	2.79	1.40
5	3.63	3.57	3.63	2.74	2.72	0.52	9.56	9.36	9.56	9.26	6.04	2.82	4.86	5.36	5.36	4.08	3.16	1.29
6	4.62	4.01	4.62	3.69	2.82	0.92	5.59	5.80	5.80	4.27	3.30	1.44	4.10	4.97	4.97	2.97	2.77	0.92
7	4.71	4.32	4.71	4.61	2.74	0.52	6.49	6.46	6.49	4.50	2.76	1.70	4.72	5.23	5.23	3.95	3.80	0.93
8	4.36	4.24	4.36	3.98	2.95	0.74	5.13	5.44	5.44	3.65	2.88	1.28	5.50	6.02	6.02	4.57	3.23	1.64
9	4.87	4.47	4.87	3.10	2.84	1.16	5.75	5.75	5.75	6.07	2.11	1.85	6.20	7.08	7.08	5.37	4.02	1.45
10	4.90	4.29	4.9	4.18	2.45	1.12	12.66	12.70	12.70	11.49	6.52	4.20	5.53	6.14	6.14	3.42	3.62	1.21
11	5.26	4.61	5.26	3.33	2.78	1.18	5.45	5.60	5.60	4.09	2.93	1.69	6.94	7.14	7.14	4.82	4.34	1.68
12	11.55	10.69	11.55	9.30	5.94	2.65	11.88	11.74	11.88	7.70	4.50	4.33	7.27	7.73	7.73	5.71	5.00	1.87
13	4.93	4.67	4.93	4.73	2.92	0.87	5.11	5.13	5.13	4.05	2.58	1.60	6.06	6.51	6.51	5.24	3.31	1.64
14	4.92	4.31	4.92	4.36	2.46	1.44	6.72	6.72	6.72	4.46	2.77	1.79	5.69	6.67	6.67	4.69	4.69	1.18
15	5.05	4.27	5.05	3.74	3.13	0.96	4.98	5.01	5.01	3.97	2.63	1.71	4.53	4.74	4.74	2.04	3.57	0.90
16	6.05	4.67	6.05	5.18	3.54	0.87	5.54	5.59	5.59	4.82	1.79	1.95	4.99	5.69	5.69	3.10	3.42	1.15
17	4.36	3.95	4.36	4.05	2.26	0.98	11.57	11.57	11.57	8.95	4.73	3.02	4.37	5.11	5.11	3.07	2.97	0.97
18	4.66	4.38	4.66	3.37	2.73	1.29	5.23	5.03	5.23	4.62	2.00	1.70	4.98	5.21	5.21	3.70	2.76	1.71
19	5.19	4.85	5.19	4.24	2.77	1.76	10.87	11.07	11.07	9.56	4.93	3.82	4.26	5.18	5.18	2.92	2.77	0.67
20	4.40	4.07	4.40	2.95	2.34	1.14	5.08	5.13	5.13	2.87	2.15	1.56	4.36	4.92	4.92	3.03	3.13	0.82
21	10.77	9.56	10.77	11.07	5.84	3.32	5.60	5.65	5.65	3.64	2.41	2.06	4.77	6.51	6.51	4.82	3.64	1.08
22	6.00	5.13	6.00	5.03	3.49	1.28							5.44	6.16	6.16	5.13	3.08	1.53
23	10.72	10.20	10.72	7.24	5.76	2.13							4.56	6.46	6.46	4.82	3.18	1.44
24	10.31	9.43	10.31	6.88	5.99	2.12							5.75	6.08	6.08	3.48	2.89	1.72
25	8.24	7.48	8.24	6.84	4.93	1.44							6.05	6.72	6.72	4.36	3.59	0.92
26	8.68	7.37	8.68	6.00	5.29	1.76							4.59	4.72	4.72	4.79	2.87	1.13
27	10.97	10.56	10.97	7.04	6.14	2.09							4.84	4.98	4.98	3.30	2.87	1.03
28	8.49	7.54	8.49	6.84	5.34	1.79							4.05	4.77	4.77	3.44	2.62	1.08
29	9.66	8.36	9.66	6.94	6.24	2.11							5.23	6.05	6.05	4.05	4.41	1.03
30	14.05	11.26	14.05	9.53	9.05	2.42							4.72	5.69	5.69	4.47	3.28	1.18
31	10.44	7.92	10.44	8.10	7.11	1.54							4.71	5.04	5.04	3.18	3.96	0.78
32	8.85	8.15	8.85	6.64	5.73	1.21							6.20	6.69	6.69	3.81	4.81	1.43
33	9.42	8.31	9.42	6.11	5.70	1.79							5.66	6.18	6.18	4.17	4.19	1.49
34	9.05	8.45	9.05	6.34	6.24	1.11							5.34	5.52	5.52	3.45	3.45	1.23
35	5.12	4.77	5.12	4.17	3.39	1.08							4.97	5.60	5.90	4.21	3.08	1.44
36	4.86	4.28	4.86	2.83	3.31	1.13							9.96	11.67	11.67	8.55	6.34	2.63
37	4.92	4.59	4.92	3.85	3.39	1.36							9.16	10.68	10.68	5.98	7.45	2.06
38	5.24	4.87	5.24	4.72	3.08	1.04							5.12	6.14	6.14	3.81	3.63	1.42
39	5.03	4.62	5.03	4.36	3.03	0.87							5.74	5.88	5.88	3.86	3.26	1.42
40	5.22	4.69	5.22	4.31	3.28	1.33							4.16	4.98	4.98	3.19	3.08	1.51
41	8.65	7.85	8.65	5.03	5.53	1.61							5.90	6.57	6.57	4.72	3.49	1.23
42													4.98	5.25	5.25	3.19	3.72	0.87
43													4.28	5.05	5.05	3.35	3.65	0.73
44													3.95	4.74	4.74	3.10	3.30	0.85
45													4.88	5.33	5.33	2.52	4.00	0.67

Appendix 1: Morphometric data for all measured specimens. All measurements are in micrometers (μm).